Missouri State University

BearWorks

MSU Graduate Theses

Spring 2016

Seismic Reflection, Well Log, And Gravity Analysis Of The Thrace Basin, Northwestern Turkey

Murat Kuvanc

As with any intellectual project, the content and views expressed in this thesis may be considered objectionable by some readers. However, this student-scholar's work has been judged to have academic value by the student's thesis committee members trained in the discipline. The content and views expressed in this thesis are those of the student-scholar and are not endorsed by Missouri State University, its Graduate College, or its employees.

Follow this and additional works at: https://bearworks.missouristate.edu/theses

Part of the Geology Commons, and the Geophysics and Seismology Commons

Recommended Citation

Kuvanc, Murat, "Seismic Reflection, Well Log, And Gravity Analysis Of The Thrace Basin, Northwestern Turkey" (2016). *MSU Graduate Theses*. 2372.
https://bearworks.missouristate.edu/theses/2372

This article or document was made available through BearWorks, the institutional repository of Missouri State University. The work contained in it may be protected by copyright and require permission of the copyright holder for reuse or redistribution.
For more information, please contact BearWorks@library.missouristate.edu.

SEISMIC REFLECTION, WELL LOG, AND GRAVITY ANALYSIS OF THE THRACE BASIN, NORTHWESTERN TURKEY

A Master Thesis

Presented to

The Graduate College of

Missouri State University

In Partial Fulfillment

Of the Requirements for the Degree

Master of Natural Applied Sciences

By

Murat Kuvanc

May, 2016

Copyright 2016 by Murat Kuvanc

SEISMIC REFLECTION, WELL LOG, AND GRAVITY ANALYSIS OF THE THRACE BASIN, NORTHWESTERN TURKEY

Geography, Geology, and Planning

Missouri State University, May 2016

Master of Natural Applied Sciences

Murat Kuvanc

ABSTRACT

The Thrace basin is located between the Paleogene the Istranca and Rhdope massifs in the northwestern part of Turkey. Sediments in the Thrace basin accumulated during the early Eocene to the late Miocene, and the basin includes normal and strike-slip faults that were mainly formed in the Miocene. The hydrocarbon potential of the Thrace basin has been investigated by analyzing seismic reflection, well log, and gravity data since the 1930s; the basin has a huge gas reservoir potential and contains the first gas production field in Turkey. To determine the geologic and geophysics features of a portion of the basin and investigate the hydrocarbon potential of that area, new seismic reflection, well log, and gravity data were analyzed here. These data provide for subsurface maps and images that show the geologic structures, which include pull-apart basin and anticlinal structure. Well log analyses shows gas-bearing zones in the Well 2 and 3 wells but these results do not support the idea that the reservoir has economic potential for gas production. Gravity anomalies were mapped to show the overall basin thickness.

KEYWORDS: Thrace basin, Turkey, gas reservoir, seismic reflection data, well log data, gravity data

This abstract is approved as to form and content

____

Kevin L. Mickus, PhD
Chairperson, Advisory Committee
Missouri State University

SEISMIC REFLECTION, WELL LOG, AND GRAVITY ANALYSIS OF THE THRACE BASIN, NORTHWESTERN TURKEY

By

Murat Kuvanc

A Master Thesis
Submitted to the Graduate College
Of Missouri State University
In Partial Fulfillment of the Requirements
For the Degree Master of Natural and Applied Sciences

May 2016

Approved:

____
Kevin L. Mickus, PhD

____
Melida Gutierrez, PhD

____
Kevin Evans, PhD

____
Julie Masterson, PhD: Dean, Graduate College

ACKNOWLEDGEMENTS

I would like to thank my committee members, Dr. Kevin Mickus, Dr. Melida Gutierrez, and Dr. Kevin Evans for their patience and support to help me finish my thesis. They have always tried to help me to solve problems about my study. I believe that these experiences which are provided by them will lead me to be wise person on my job and rest of my life. Especially for Dr. Mickus, he has accepted me to the master program at the Missouri State University and guided through my studies.

I would also like to thank Turkish Petroleum Corporation which provided seismic reflection and well log data for my study. My colleagues at the Turkish Petroleum Corporation have answered many of my questions to make some of processing steps successfully. Moreover, I want to send thanks to Dr. Douglas R. Gouzie who is the Departmental Director of Graduate Studies and the Geography Geology and Planning Department for his help.

I would also like to thank my parents Emine and Bunyamin Kuvanc, my sisters and my friends. Especially, my fall in love wife who is Rabia, my mother, and my father have supported and encouraged me whenever I needed it, and I believe that I would not have achieved anything without their love.

TABLE OF CONTENTS

LIST OF TABLES

LIST OF FIGURES

INTRODUCTION

The Thrace region is located in the border of Turkey, Greece, and Bulgaria, and the region is known as the Thrace basin on northwestern side of Turkey (Figure 1). The basin which covers a 16,835 km^2 area (6,500 mi^2) has a triangular shape located between Istranca on north, Rhodope on west, and the Menderes massifs in the south. The basin started to form in the Early Eocene time and has continued to grow until recent time (Perincek et al., 2015). The sedimentation rate within the basin was accelerated by Miocene age tectonism. Normal and strike slip faults accommodated up to 9,000 meters of sediment at places in the basin (Derman, 2014).

During Miocene time, Eurasia was subjected to intense tectonic activities including plate motions between Europe and Africa that produced the South Alpine thrusting, and the Tethys Sea that was located between the Mediterranean Sea and Indian Ocean was separated. Also, Miocene tectonism caused severe deformation with strike-slip movements in the basin especially for southern region (Conybeare et al., 2004). In the Thrace basin, normal and strike-slip faults are located within numerous fault zones including the Kirikkale, Luleburgaz, Babaeski, and also the North Anatolian Fault system (NAFs; Derman, 2014). These fault zones, especially the NAFs, significantly affected the basin. Fault zone deformation caused multiple geologic structures such as anticlines and pull-apart basins which are formed after strike-slip motions (Siyako and Huvaz, 2007).

The Thrace basin, which is the largest Cenozoic-age sedimentary basin in Turkey, contains a high volume of petroleum reservoir and source rocks, it has been drilled extensively since the 1970’s. Exploration has produced useful results together with the

many wells that were drilled and produced data to identify the basin's geologic features (EIA, 2015). Siyako (2006) and Coskun (1996) investigated the Thrace basin's tectonic features and Keskin (1971) studied the sedimentology of the basin. According to these studies, geological traps were formed as a result of high tectonic activity accompanied by massive sedimentation.

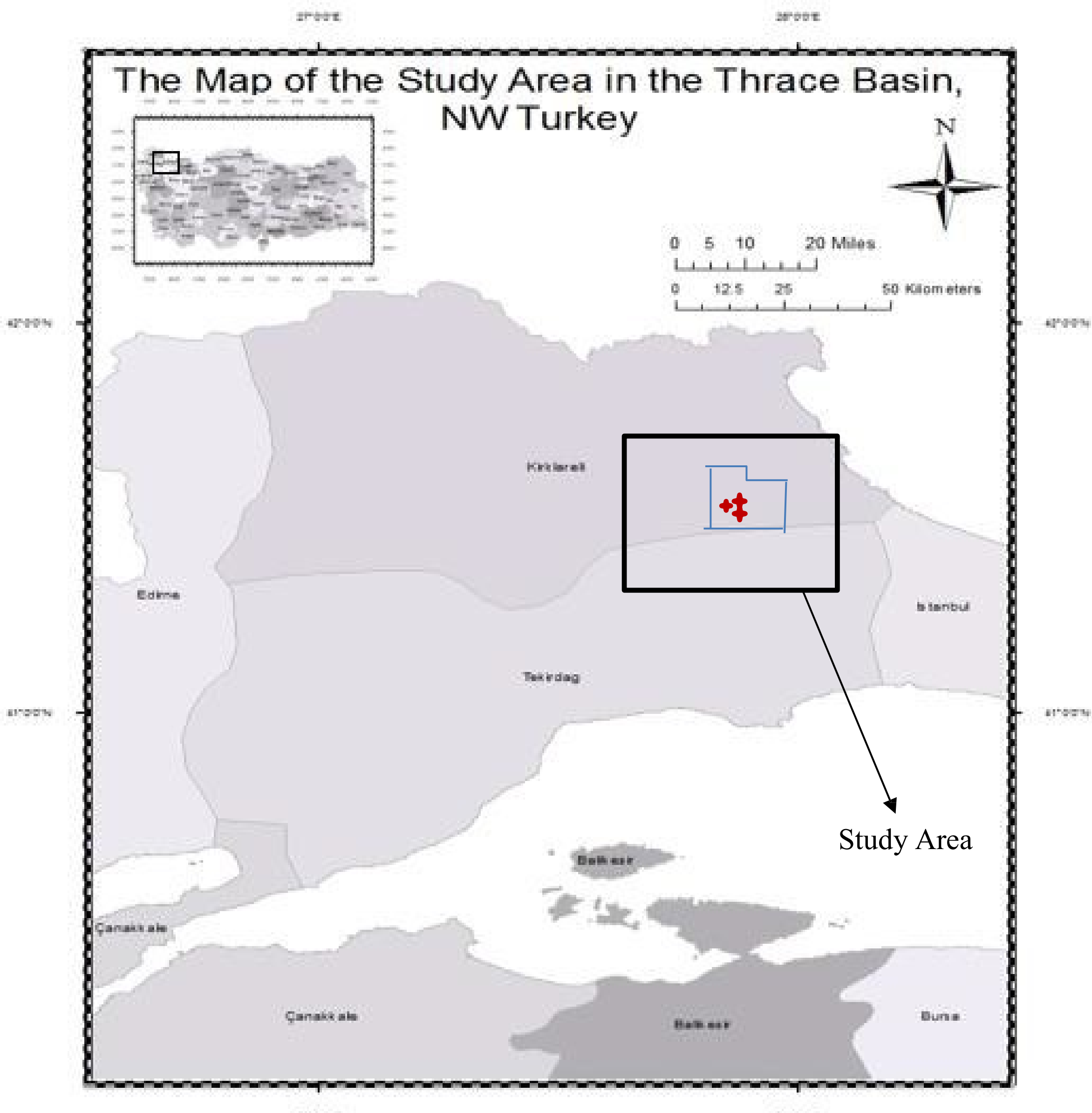

Figure 1. Location of the study area showing the location of three dimensional (3D) seismic reflection and well logs field data in the Thrace basin in Turkey. Blue polygon shows the 3D seismic survey, red symbols are Well 1 2 3 wells.

The Thrace basin is the main gas producing region in Turkey with 85% of the total gas production of Turkey. The sources of the gas in the Thrace basin are tight sand and shale rocks (EIA, 2015).The shale potential of the Thrace basin is also suitable for the new technique to exploit unconventional natural gas deposits using horizontal drilling and hydraulic fracturing in the shale formations recommended by American Petroleum Institute (API). Therefore, the Turkish Petroleum Corporation (TPAO) and other companies (Trans-Atlantic, Shell etc.) have started to apply the shale gas technique to improve their production artificially from shale formations which are generally from the Mezardere and Hamitabat Formations.

According to data from the TPAO, the petroleum producing formations within the study area include the Oligocene-aged Danismen and the Osmancik Formations which will be described in detail below. Moreover, the Mezardere Formation is also described briefly due to its potential for shale gas potential and since these three formations generally occur together.

Due to the fact that the Thrace basin has hydrocarbon production potential, it has to be analyzed with geophysical and well log methods. The geophysical analysis of the Thrace basin includes seismic reflection, well logs, and gravity data. The 3D seismic reflection field data which was collected and processed by TPAO was studied and modeled to interpret geological features of the basin. To improve the quality of the study, well log data was analyzed for hydrocarbon potential of the basin and was interpreted in conjunction with the seismic and gravity data.

CHAPTER 1

1.1 Tectonic and Structural Settings of the Thrace Basin

The Thrace basin is positioned between the granitic and mica schist rocks of the Istranca (Strandaja) and Rhodope Massifs (Figure 2). The formations of the Thrace basin resulted after the Anatolian and Arabian plates collision along the southeast part of Turkey during Maastrichtian time. The Thrace basin was displaced by strike-slip motion along the Anatolian fault to the northwest and this deformation created horst and graben structures in the Anatolian plate. The basin which has a triangular shape is thought to be a forearc basin due to the subduction on its north side (Coskun, 1996; Kilias et al., 2011).

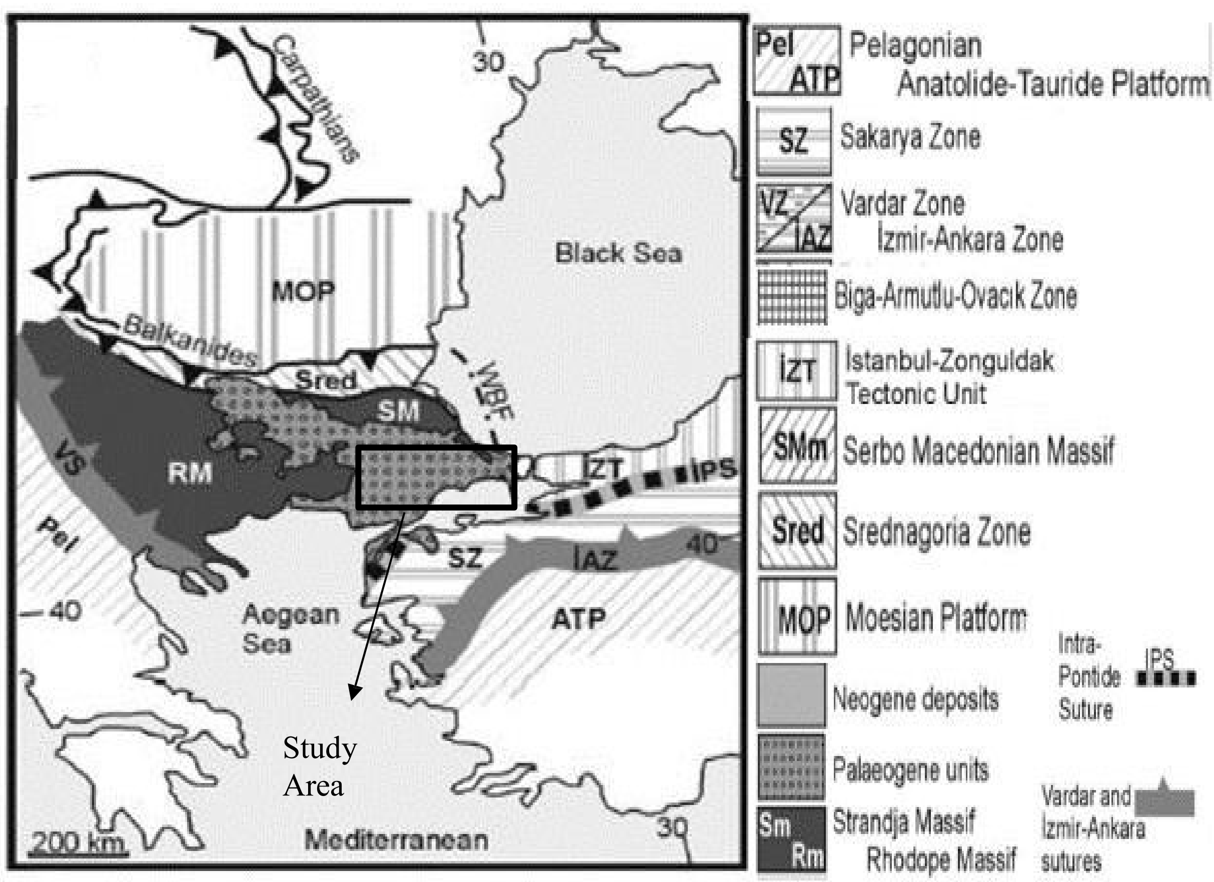

Figure 2. Geological map of the Thrace basin between the Strandja (SM) and Rhdope (RM) massifs (modified after Elmas, 2011).

Much of the tectonic movement between the African, Anatolian, and Eurasian plates occurred during Maastrichtian and Miocene times within the Thrace basin region. The geologic, stratigraphic, and tectonic features associated with these plate motions were first investigated in the early 1930s (Elmas, 2011: EIA, 2015). Deposition within the basin occurred between the Rhodope-Strandaja Massif and is located in the west and north sides of the basin, and the Biga peninsula that is located in the basin's southern part (Figure 3; Gorur and Okay, 1996).

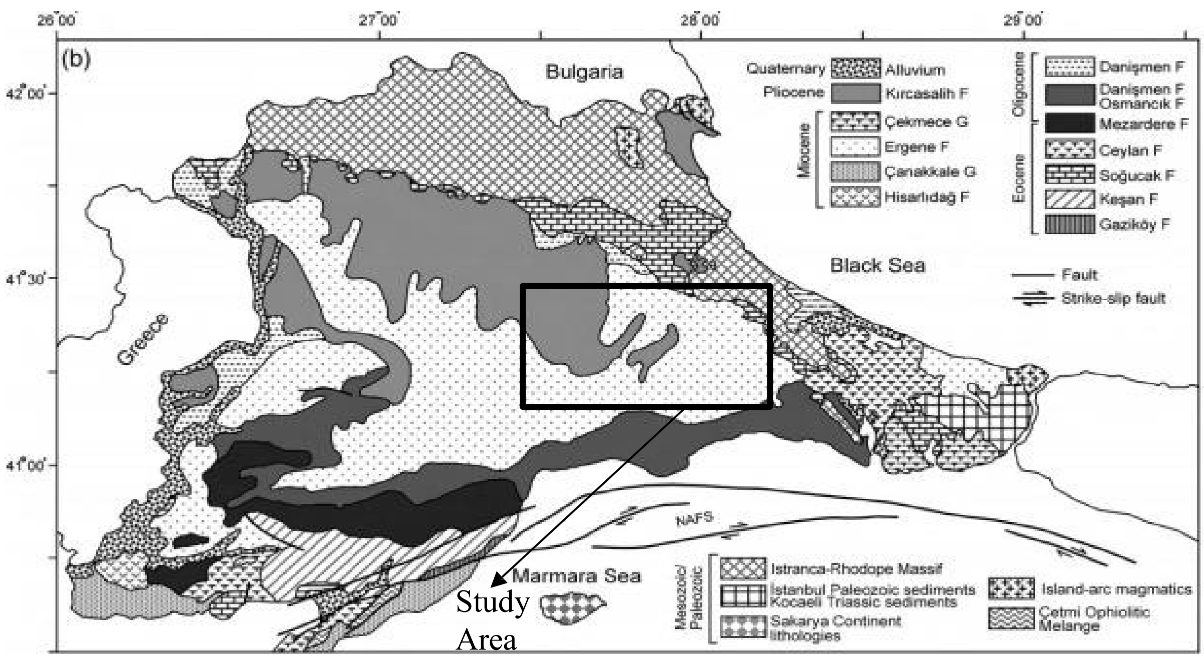

Figure 3. Map of the tectonic and stratigraphic features of the Thrace between the Istranca and Rhdope massifs (modified after Siyako and Huvaz, 2007).

The southern margin of the basin contains several different geological features. This region experienced deformations including anticlines and normal faults formed by the movement of the North Anatolian Fault, and it is now covered by the Marmara Sea (Datri et al., 2012). The Thrace basin in this region can be defined as a depo center with the thick accumulation of sediment that occurred in this tectonic setting; it is the largest

and thickest basin in the eastern part of the Balkan region. (Turgut et al., 1983). There are Plio-Quaternary deposits in the center of the basin and also in the northern part of the basin, which can be seen near the basin border (Siyako, 2006). Most of the sedimentary units within the basin date from the lower Eocene to Upper Oligocene. The main sections of the basin are approximately 5,000 meters deep and reach up to 9,000 meters in thickness in some places adjacent to strike slip faults (Yildiz et al., 1997).

The Cenozoic-age sediments within the Thrace basin were deposited as a delta that is now underlaid by and confined within the three massifs. These massifs are: in the north the Istranca massif, in the west the Rhodope massif, and in the south the Menderes massif (Figure 4; Usumezsoy, 1982; Derman, 2014). The Istranca massif has nearly 300 kilometers long and 40 kilometers wide, and contains up to 10 kilometers thickness of Tertiary sediments. The Istranca massif is composed of Triassic and Middle Jurassic-Triassic age phyllite, slate, metabasite and metasandstone, and lower Permian age metagranitoids (Bedi et al., 2013). The boundary between the Rhodope massif and Thrace basin is located in the western part of Turkey but the main part of the Rhodope massif is located in Greece. The Rhodope massif includes mainly high to medium grade metamorphic units formed during PreAlpine and Alpine collisional tectonics (Kilias et al., 2011). The Menderes massif is composed of mainly metamorphic and igneous rock units which were formed during Alpine and Pan-African orogenies (Hinsberger, 2010)

The subduction of the African plate under the European plate was the ultimate cause of the Thrace basin (Saner, 1980; Sengor and Yilmaz, 1981) with the basin being modified by later strike-slip faulting along the Northern Anatolian fault. Expansion occurring during Late Middle Eocene to Latest Oligocene time resulted in further

sediment accumulation (Keskin, 1974). The normal fault systems associated with the base of the basin allowed the accumulation of up to 9,000 meters of clastic sediments (Derman, 2014). The basin expanded toward the north in the Late Eocene by further collision tectonics so the large northern region of the basin was formed. Also, the shelf region in the northern parts of the basins was shallow enough so that carbonates were deposited during this time.

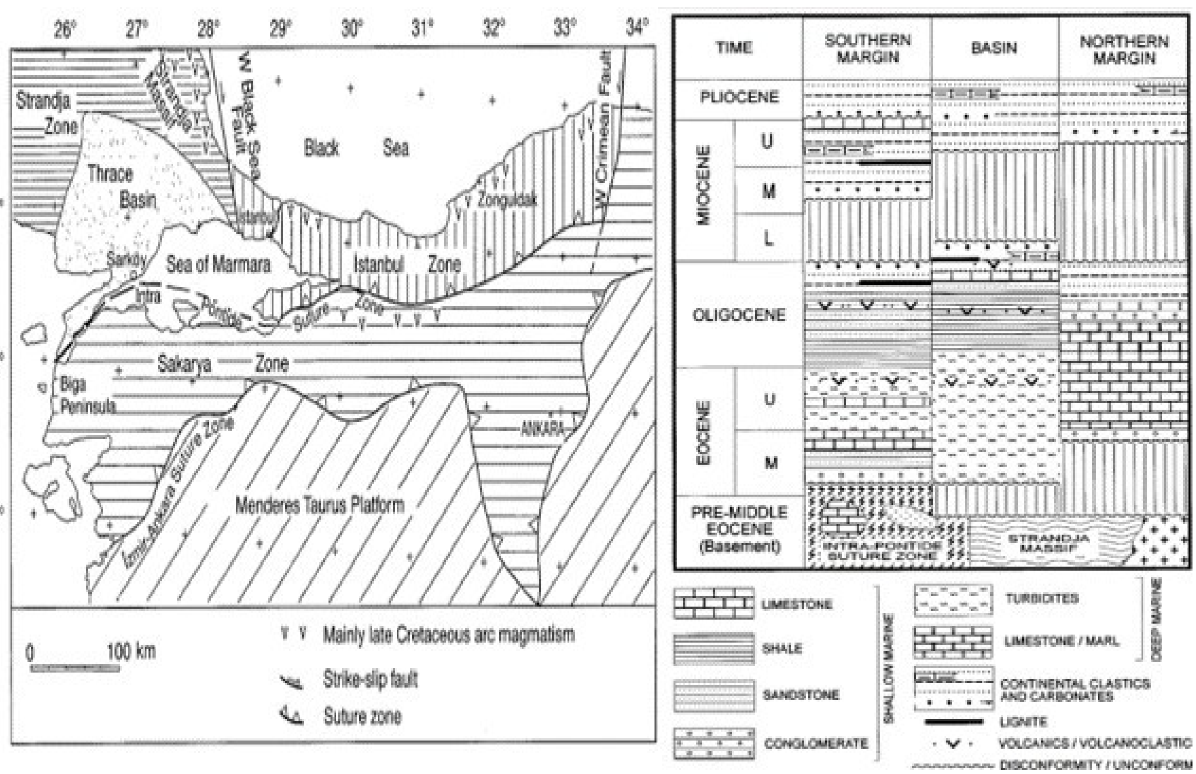

Figure 4. Geological map of the Thrace basin (left), and stratigraphy of the Thrace basin (right) (modified by Gorur and Okay, 1996).

Geologic Formations within the Thrace Basin. The Thrace basin basement lithology which ranges in age from Precambrian to Triassic includes the Istranca massive, Rhodope massive metamorphic, Istanbul Paleozoic, Kocaeli Triassic sediments, and Cetmi Ophiolitic Mệlange (Figure 5; Derman, 2014). Metamorphic rocks that crop out in the northern side of basin are exposed in the Istranca Mountains next to the NAFs. Paleozoic rocks underlying and surrounding Istanbul are named the Istanbul Paleozoic

sequence. The Istanbul Paleozoic units have been intruded in many places by volcanic dykes and diabases. These volcanic intrusions have been interpreted to have been caused by a single magmatic phase but there is no adequate information about their structural features, geochemistry and geochronology. Kocaeli Triassic sediments are exposed in the east side of the basin (Siyako and Huvaz, 2007; Sen, 2011; Derman, 2014).

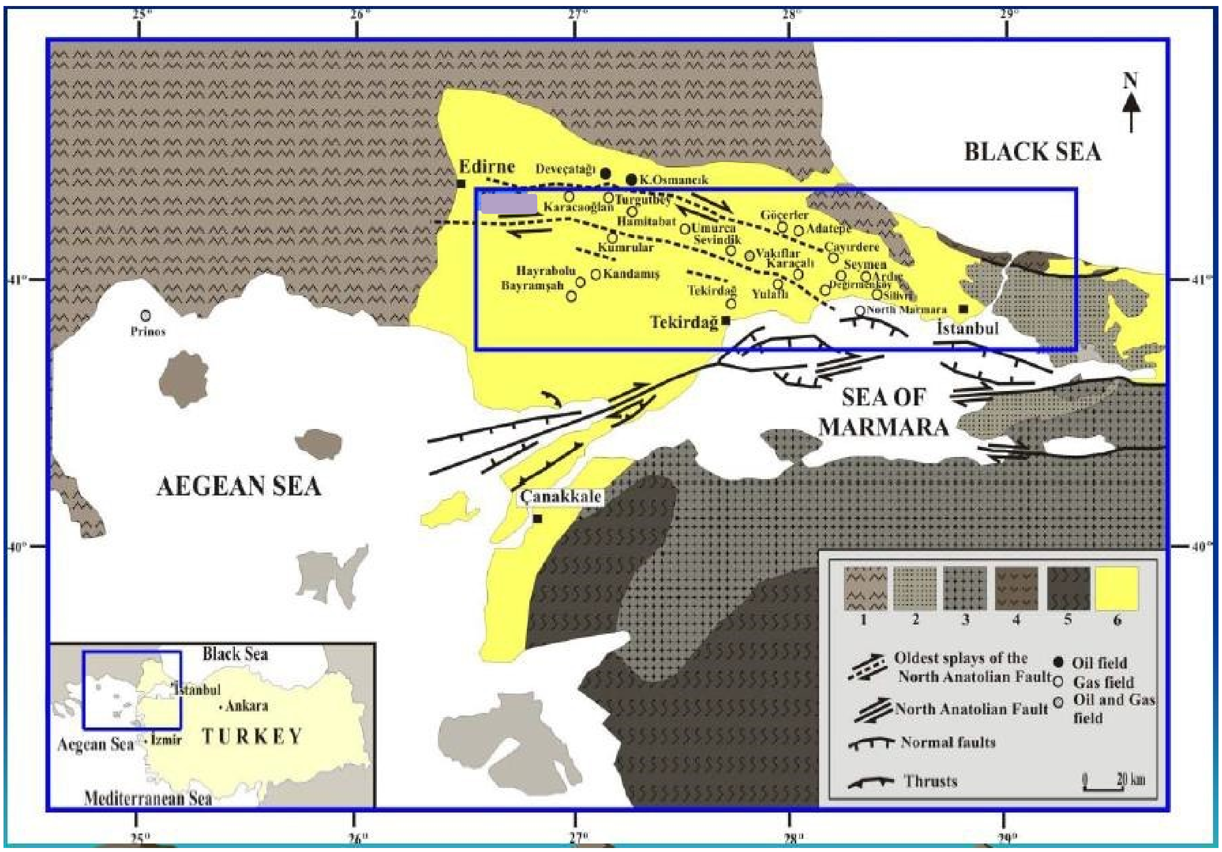

Figure 5. Geologic formations within the Thrace basin. 1) Istranca Massive, 2) Istanbul Paleozoic sediments, 3) Paleotethys remnants, 4) Upper Cretaceous arc volcanics, 5) Neotethys subduction-accretionary complex, 6) Thrace Basin sediments. (modified after Sen, 2011)

The Osmancik Formation. The Oligocene-aged Osmancik Formation extends from northeastern Kesan to Tekirdag and to Istanbul, and within the Thrace basin it also named the Danismen Formation because it grades into the Danismen Formation laterally. The Osmancik Formation generally is located under the Danismen Formation and above the Mezardere Formation, and the Osmancik Formation frequently forms a gradational

contact with both. Thus, there is a problem to decide where the formation base and top should be placed, especially the boundary between the Osmancik and Danismen Formations (Figure 6).

Sandstones within the Osmancik Formation are fine to medium grained, showing occasional friability and immaturity, and are 100-150 meters thick. The Osmancik Formation has traces of lignite. However, the thickness and distribution of lignite in the Osmancik is less extensive than those within the Danismen Formation. According to drilled wells, the entire formation consisting of sandstones and shales is nearly 800 meters (2,624 feet) thick. The fossils in the basin are generally of Oligocene age (Turgut et al., 1983; Temel and Ciftci, 2002).

The Danismen Formation. According to well logs, the Danismen Formation is present in the northern Thrace basin. The formation extends up to the Yildiz (Istranca) Mountains that is located in the north side of the Thrace basin and also crops out in the south side of the basin (Siyako, 2006). It includes green-grey shales, claystones, and siltstones, and its thickness is nearly 200 meters but it reaches up to 1,000 meters in places. The thickness of formation gets thinner towards the edge of the basin. The Danismen Formation is Oligocene in age and is similar in nature to the Osmancik Formation (Coskun, 1996). There are graded transitive boundaries between the Danismen and Osmancik Formations. The Danismen Formation is eroded in the upper part, and is covered with an unconformity (Figure 6; Siyako, 2006).

The Mezardere Formation. According to field data, the Mezardere Formation was not identified in the study area but it is generally present near the other two formations. Thus, the general features of the Mezardere Formation are briefly explained

here. The Mezardere Formation is placed under the Osmancik Formation throughout the Thrace basin. It is under both the Danismen and Osmancik, and has a transitional less boundary with the Osmancik Formation. It is about 600 meters thick, and includes dark grey black shales, sandstones that are good grained, and siltstones. Black shales are useful petroleum source rocks and as unconventional reservoirs (Figure 6; Unal, 1967).

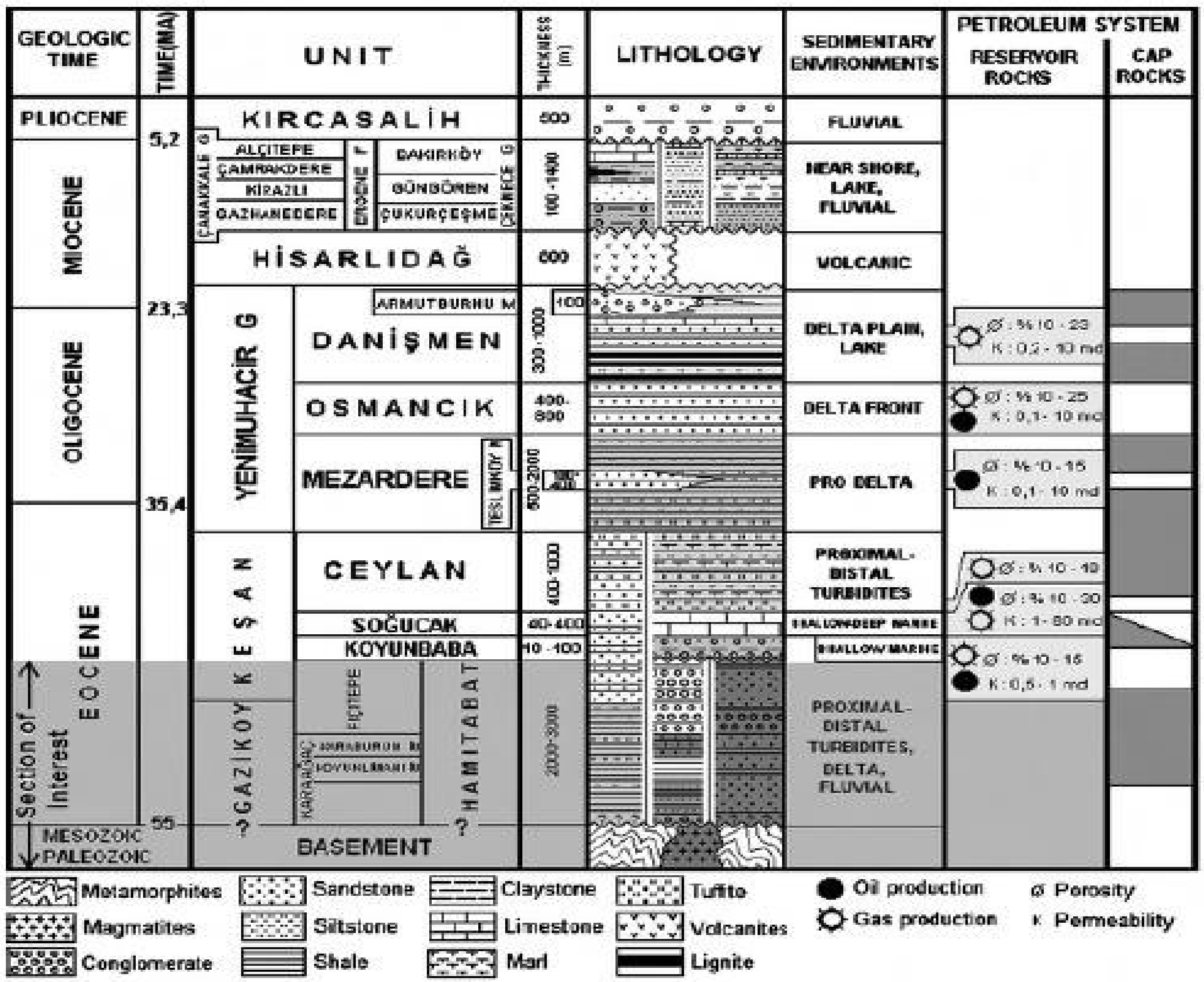

Figure 6. Stratigraphy of oil-producing units in the study area (modified after Siyako and Huvaz, 2007).

Fault Zone Systems. Faults zones within the Thrace basin include: the Kirklareli, Luleburgaz, and Babaeski. Kirklareli fault zone is dominant features. The north side of basin has normal faults but the east side of the fault turns to a positive flower structures

formed by strike-slip faulting (Perincek, 1991). This latter fault zone may have affected the Osmancik and Devecatagi oil fields. The Luleburgaz fault zone, found in the south side of the Kirklareli fault zone, has both positive and negative flower structures, and is located under Umurca and Hamitabat oil fields (Perincek, 1991). There is not enough information about the Babaeski fault zone, and it has not been mapped in detail (Figure 7).

The Babaeski fault zone has had right-lateral movement and might be associated with volcanic activity that is known to affect the thermal overprint in the basin (Derman, 2014). The southern side of basin has suffered large amounts of deformation caused by Miocene tectonism. The basin's marginal fault systems are associated with the northern side of the basin, whereas wrench faults system are associated with the middle of the basin. These fault systems affect in great manner the structural petroleum traps. These structural traps are important for hydrocarbon production, therefore production is more intense in the northern margin and north central parts of basin (Perincek, 1991; Turgut et al., 1991; Derman, 2014).

Flower Structures. The Miocene-aged North Anatolian Fault system caused right-lateral wrench movements within the Thrace basin. Seismic reflection profiles indicate flower structures that have a NW-SE direction are related to these movements (Coskun, 1996).

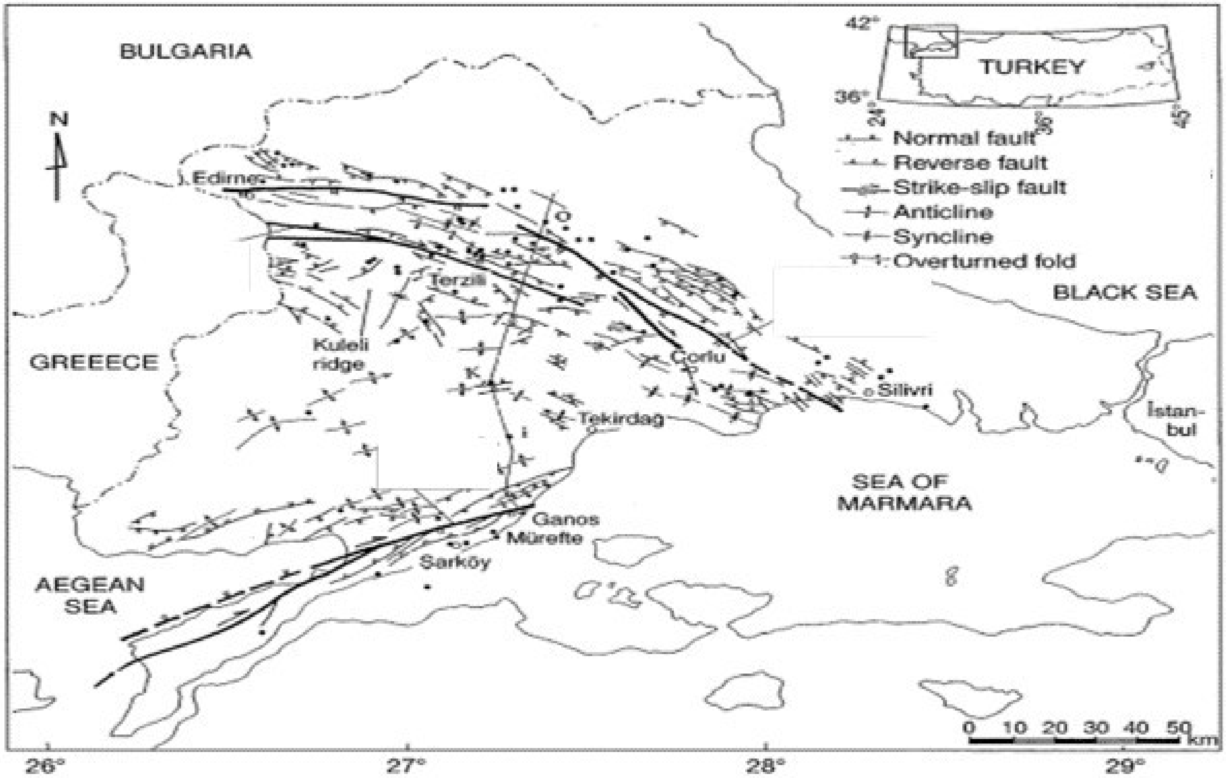

Figure 7. Structural features of the Thrace basin (modified after Gorur and Okay, 1996)

1.2 Petroleum Geology of the Study Area

Depositional Model. The Thrace basin depositional model is related to middle Eocene and Miocene tectonics because the basin started to be form along the NE-trending western Marmara sea ridge that is parallel to the central Marmara ridge within the Marmara Sea. Also, the NAFs affected this region in the Late Miocene period (Figure 8; Schindler, 1997). These tectonic events might be main reason for the characterization of the Thrace basin sedimentation, which include turbiditic, deltaic, and fluvial phases. In Eocene-Early Miocene time, basin sedimentation was increased but the depositional rates decreased by middle Miocene-Pliocene time. However, there is less information about the lower-middle Eocene time sedimentation because of an insufficient bio-stratigraphic record (Siyako and Huvaz, 2007).

The Hamitabat Formation, which underlies the Mezardere Formation, was deposited in a turbiditic environment. Sandstones in the Hamitabat do no extend everywhere in the Thrace basin. This type of sandstones includes good porosities (12-15%) and permeabilities (approximately 100 md) and have a potential for gas production (Coskun, 1996).

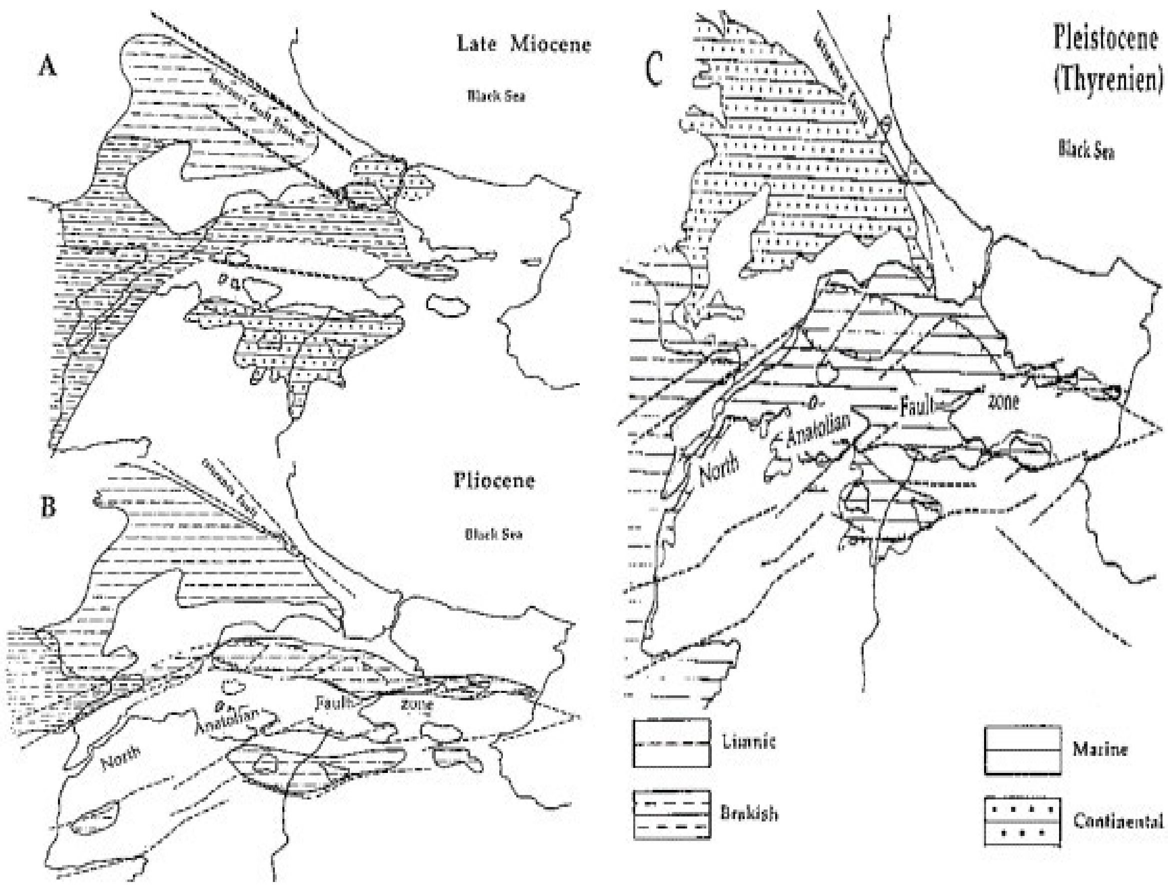

Figure 8. Paleogeographic maps of the Marmara sea region that include the Thrace basin. The basin sedimentation was affected by the Marmara sea ridge and the NAFs (modified after Schindler, 1997).

The prime gas producers in the basin are sandstones that were deposited in a delta front setting. Also, the fluvial facies include intercalated sands and conglomerates, which are at angular discordance with formations below (Coskun, 1996). The deltaic phase occurs after the turbiditic phase. This phase is represented by the Mezardere Formation and includes sandstones, shales and conforms to a prodelta cycle. It contains dark grey

shales, and these shales are source rocks in the formation (Coskun, 1996). On the other hand, the Osmancik Formation that is generally located over the Mezardere Formation conforms to the delta front portion of the basin-fill succession. The Osmancik Formation is composed of sandstones that are coarse, white to grey colored, porous and permeable, and slightly immature (Coskun, 1996).

Source Rocks. The Thrace Basin is a producer of petroleum with numerous gas and oil deposits located throughout the basin. Oil production generally occurs from the Oligocene-aged shales and the Eocene-aged siliciclastic rocks, and these siliciclastic rocks also have gas production potential (Burkan, 1992). According to Burkan (1992), the TOC (Total Organic Carbon) values in the Eocene unit are between 0.01% and 6.37%, and the Eocene has type I and type II kerogen in the Osmancik and Mezardere Formations. However, Soylu et al. (1992) claim that the Early to Middle Eocene Formations in general include types III and types I, and the Late Eocene has type III (Burkan 1992; Soylu et al., 1992). Type III kerogens tend to be gas prone (Van Krevelen, 1984).

The maximum maturity within the shales has been reported in the central part of basin, and also its hydrocarbon status is over-mature (Soylu et al., 1992). However, less mature hydrocarbons are present in the south side of the basin (Burkan 1992). Many of the sediments that formed in the Middle to Early Eocene have a low gas and oil potential. However, it is hard to calculate the amount of the over-mature and mature deposits and the possible gas or oil potential of the formation is not known exactly but many of the immature deposits include huge amounts of organic material that have not been converted to hydrocarbons (Derman, 2014).

Reservoir Rocks. The Thrace basin has an abundance of reservoir rocks that here will be classified by their age. The youngest unit is the Early Eocene turbiditic sandstones that form the base of the Eocene units, and also includes deltaic sandstones, reef carbonates, prodelta sands, with the oldest unit being the Late Eocene-Oligocene sands (Perincek, 1991; Turgut et al., 1991; Derman, 2014). These rocks have in general more than 10% porosity values. For example, 10 – 18 % porosity values are found in the turbiditic sandstones. However, permeability values can be different, and vary from 0.1 to 80 millidarcies (md). The Oligocene-Early Miocene prodelta sands have permeability values between 0.1 and 10 md (Siyako and Huvaz, 2007; Derman, 2014). Potential gas production units are Oligocene-Early Miocene sands, Late Eocene and Middle Eocene-Oligocene carbonates. Both gas and oil generation units are Oligocene sand and Late Eocene clastics, and also the Late Eocene –Oligocene units are capable of oil generation (Siyako and Huvaz, 2007; Derman, 2014).

1.3 Petroleum Features of the Basin

The most important reservoir rocks are Cretaceous carbonate-rich mudstones. Their general porosities are low but fractured rocks have relatively large porosity. When Miocene and Cretaceous thrusting affected the area, the mud-dominated carbonates developed highly fractured units (Derman, 2014). The secondary basin unit is found in the shallow portions of the northern part of the basin and is comprised of Late Cretaceous carbonates (Derman, 2014). The shale gas potential of the Thrace basin is related to the total organic content, depth of burial and thermal maturity. There are two shale source

rocks, which are the middle Eocene Hamitabat and lower Oligocene Mezardere Formations (EIA, 2015).

In some wells, for example Well 1, Well 2, and Well 3, the basement varies between 1,400 meters to the center of the basin where there is the nearly 4,000 meters thick sediments belonging to the Osmancik Formation. According to the above wells, the upper part of the Paleozoic section is likely to be deformed and it is characterized by an arkosic facies; this section includes gas accumulation. The Paleozoic Istranca and Rhodope massifs contain green and white mica schists, granites and black pyritic phyllites. These rocks might be the provenance for the Eocene Hamitabat and Oligocene Osmancik sandstones. These sandstones are the prime gas producer in the study area (Coskun, 1996; Derman, 2014).

CHAPTER 2

2.1 Oil and Gas in Turkey

Oil and gas account for about 64 % of the total world energy consumption (EIA, 2015). Oil and gas exploration and recovery are economically valuable but complex tasks. Imaging the subsurface for exploration is highly expensive. With a privileged location, Turkey is well positioned to distribute oil and natural gas from Russia, and the Middle East to Europe markets (Figure 9). Thus, Turkey has become a major transit hub for oil and even more important transit point for natural gas. Also, it is easy to reach oil and gas for Turkey own consumption because of its location.

Moreover, the Caspian region located between Russia, Iran, Azerbaijan, Kazakhstan, and Turkmenistan is one of the oldest oil-producing areas in the world. In recent years, the Caspian Sea oil has been carried from the Black Sea ports to mainly the European markets by oil tankers through the Turkish Straits that are Bosporus and Dardanelles, and also there are pipelines to carry Caspian Sea and northern Iraq oil across Turkey (Figure 9; EIA, 2015).

Turkey is not an oil and gas rich country and on average it imports more than 90% of its total liquid fuel from other countries. Petroleum production was less than 70,000 b/d, and Turkey's total liquid fuels consumption averaged 712,000 b/d in 2014. In 2014, most of Turkey's crude oil imports came from Iraq and Iran, and the amount of imports was nearly 87% of the Turkey's crude oil needs (Figure 10; EIA, 2015).

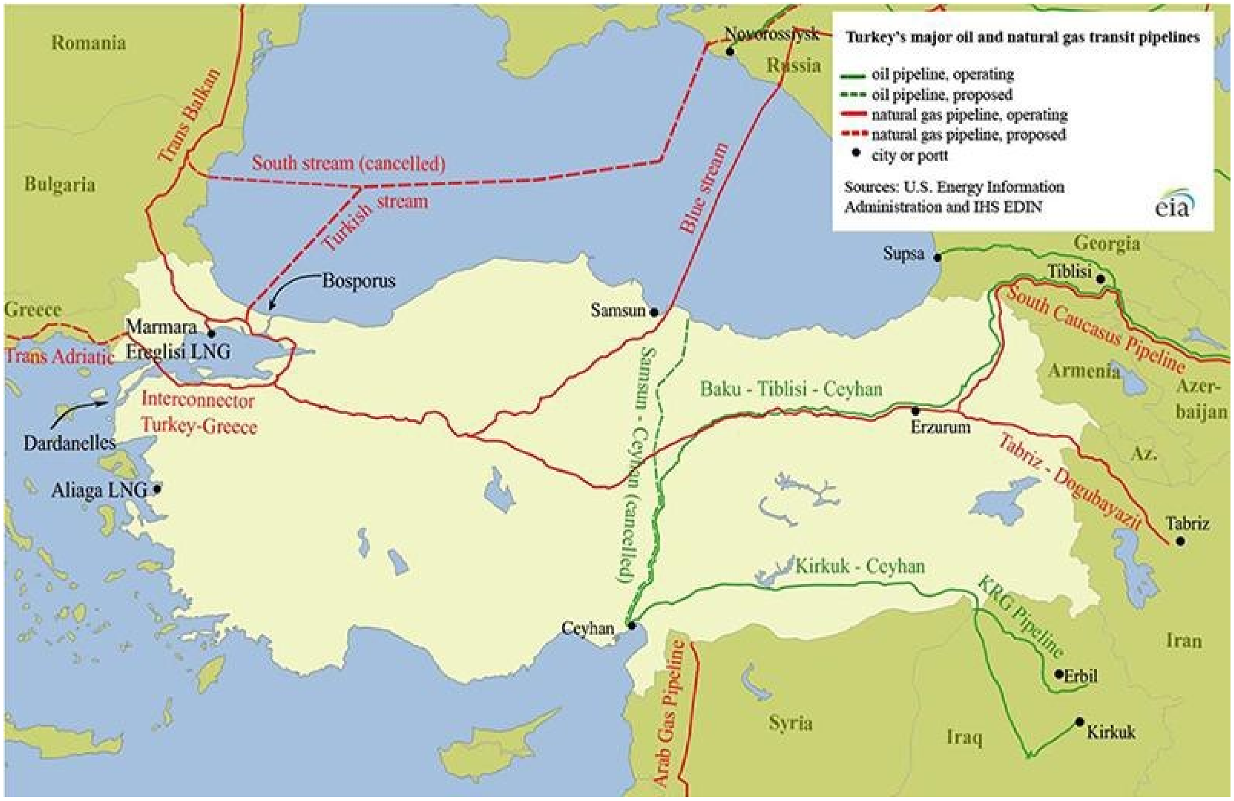

Figure 9. Major oil and gas pipeline in Turkey (taken from U.S Energy Information Administration)

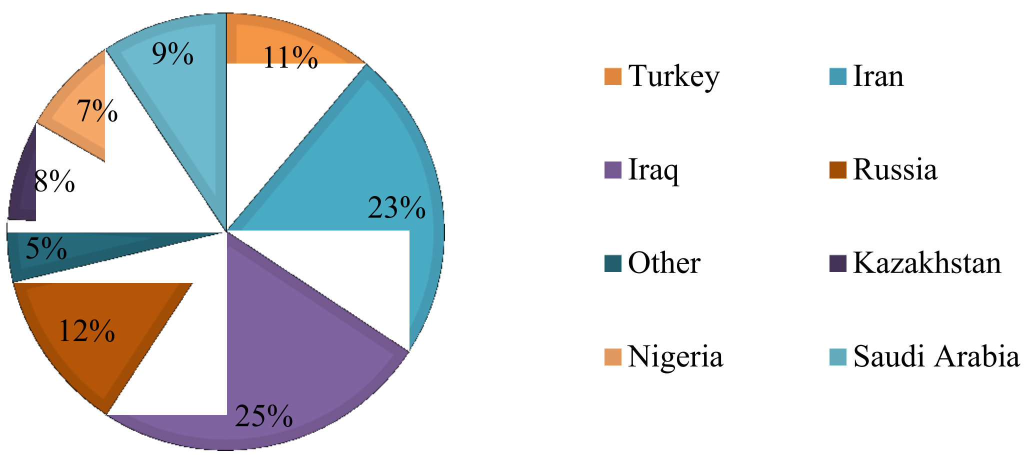

Figure 10. Crude oil supply for Turkey in 2014 (EIA, 2015).

As stated by the International Energy Agency (EIA), the amount of crude oil imports is expected to double in the next decade. Turkey only has about 270 million

barrels of proven oil reserves and 218 billion cubic feet of natural gas reserves (Figure 11).

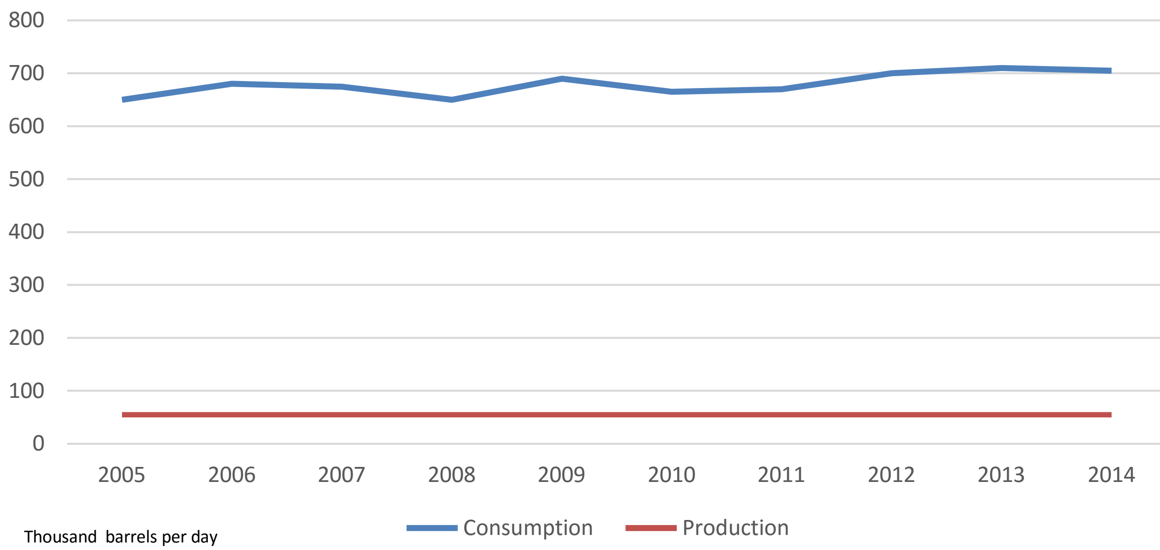

Figure 11. Petroleum and other liquids consumption and production in Turkey (EIA, 2015)

TPAO generated 12.3 million barrels of crude oil that is 72% of the total crude oil production in Turkey from the fields which were licensed in 2014. The amount of the total oil production comes from several regions including: the Batman Region (73%), the Adıyaman Region (26%), and the Thrace Region (1%). Also, on average 33,602 barrels oil per day in 2014 were produced. For natural gas production, TPAO produced 251.8 million sm³ (7 579 687.5 cubic feet and or 1.8 million barrels), and this t came from Thrace Region (95.6%), Batman Region (4.2%) and Adıyaman Region (0.2%) (Figure 12; TPAO, 2015).

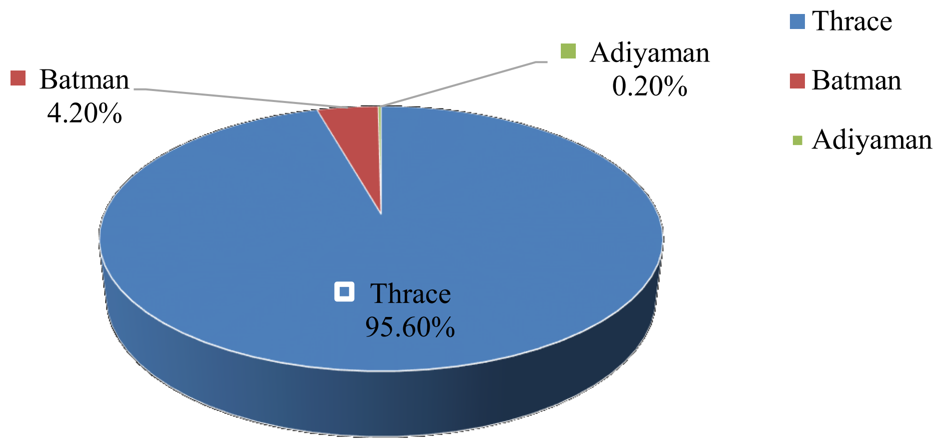

Figure 12. Natural gas production area in Turkey.

2.2 Oil and Gas in the Thrace Basin

The Thrace basin is the most important gas producing basin in Turkey with a total daily production is around of 60 Million standard cubic feet per day (MM SCFD) by three companies, (TPAO, Thrace Basin Natural Gas Company and Zorlu Energy) (Figure 13). The basin has been studied since 1950 by oil companies and academic geologists because it has vast amount of natural gas potential. Most of the parts have been searched and analyzed with well logs and seismic data because there is a thick alluvial cover that is nearly one kilometer. TPAO has investigated the oil and gas potential of the Thrace Basin since 1970. There are over 400 wells drilled, 19 gas-condensate and 3 oil fields have been discovered in the Thrace Basin. There have been many geological studies related to the Thrace Basin because of its importance in gas and oil production, and underground gas storage fields (Gorur and Okay, 1996; Okay et al., 2000; Siyako and Huvaz, 2007; Gurgey, 2009; Sen and Yillar., 2009; Islamoglu et al., 2008).

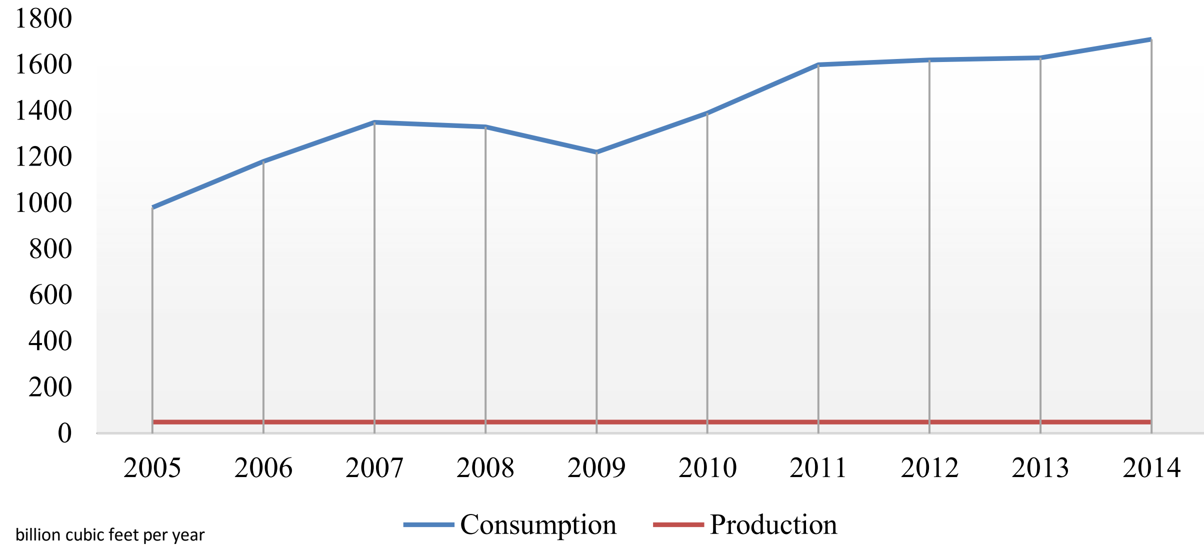

Figure 13. Natural gas production and consumption of Turkey between 2005 and 2014 (EIA, 2015).

CHAPTER 3

3.1 Reflection Seismic Method

Reflection seismology is one of the most important techniques in defining general geologic structures and depositional features that may be associated with hydrocarbon accumulations. The main idea of all seismic methods is the propagation of elastic waves from one or more seismic sources and their interaction with subsurface acoustic impedance contrasts, which can generate an image of the subsurface features. Elastic waves in the form of compressional waves (P-waves) are pulses of energy which can travel both in solids and fluids (Schuck, 2007; Patel et al., 2008) and are recorded as a function of time. The velocity of the seismic wave depends on the elastic properties of the material they travel through including lithology, porosity, saturation, pore fluids, and temperature (Kim et al., 2013; Lu, 2014).

The seismic reflection method consists of three steps: data collection, processing and interpretation (Yilmaz, 1987). Seismic data collected from the Thrace basin were received already processed, so there was left only the seismic data interpretation in this study.

The quality of data has to be taken consideration, especially for interpretation. There are three parts to data quality: detection (signal noise rate), resolution, and image fidelity (Herron, 2011). Since the aim of the seismic methods is to have interpretable data to image the subsurface, without the appropriate data quality, interpretations are specious.

3.2 Seismic Data Acquisition and Processing

In seismic data acquisition, the seismic data was collected by TPAO in a three-dimensional fashion on the northeast side of the Thrace basin (Figure 14).

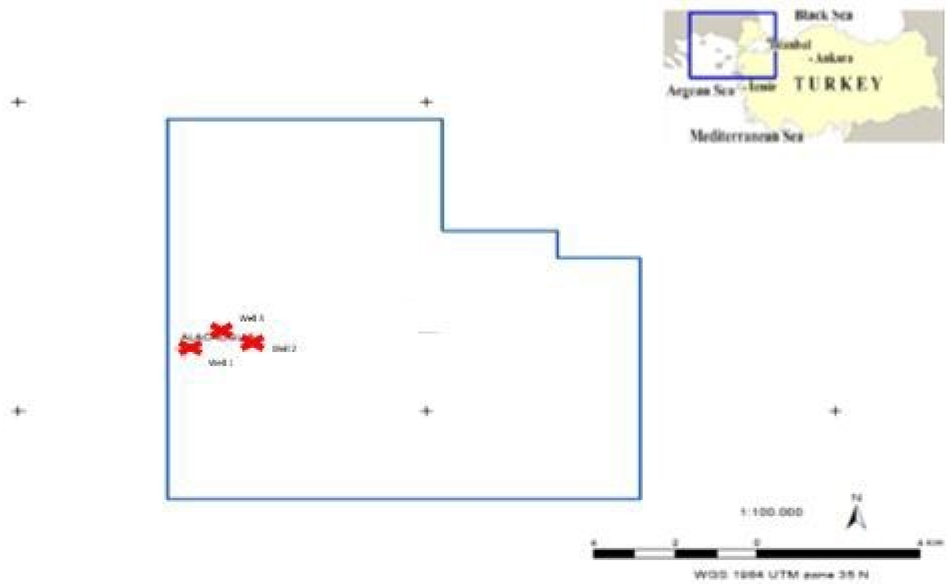

Figure 14. The seismic and well log data that were collected in the study area. Red points show wells, and the blue area is the study area were the seismic reflection data was collected.

The three dimensional seismic data were collected using the SERCEL^{TM} seismic acquisition system in 2006 (Figure 15). The data collection included the following field parameters:

- Seismic source: Dynamite
- Geophone order: 1*24 INLINE
- Distance of the geophone lines: 300 m.
- Distance of the shot lines: 400 m.
- Number of channel on a line: 128
- Total channel number: 768

- Duration of record: 5 secs.
- Sampling interval: 2 msec.
- Group interval: 50 m.
- Shot interval: 50 m.
- Number of total shot: 5445
- Total area: 123,038 Km^2

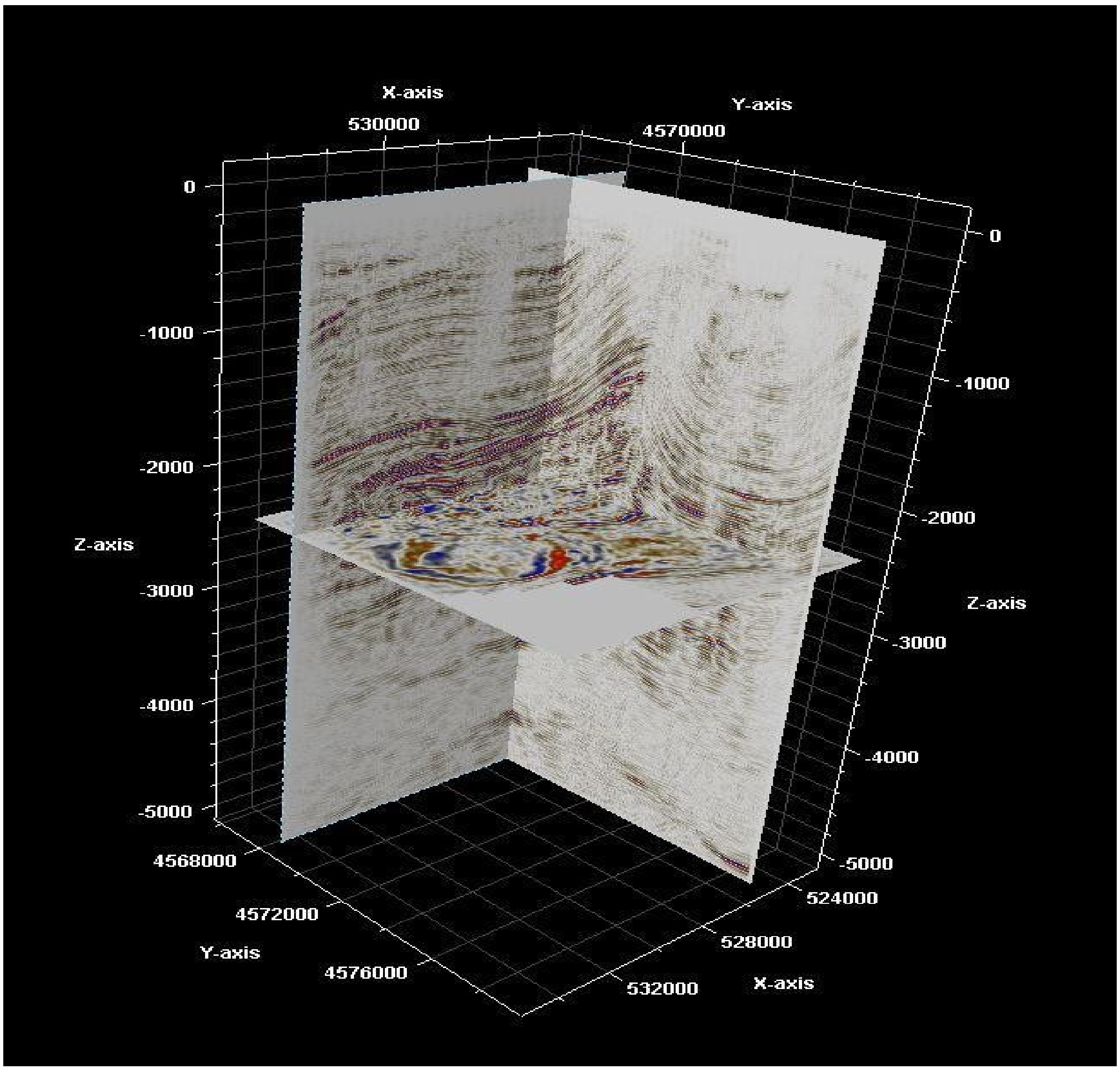

Figure 15. An example of the seismic reflection data which includes x-line, in-line and z-line slice. The z-axis is in milliseconds two-way travel time (twt), and the distances are in meters.

The field data were required several processing steps in order to interpreted. Seismic data processing mainly involves enhancing the data using a variety of methods to transform the raw data into a dataset that is suitable for seismic interpretation. The most important processing steps are to enhance the amplitudes of low amplitude reflectors and to remove noise. These low amplitudes cause the signal-to-noise-rate to be low (Hart, 2000). For this reason and to remove artifacts (e.g., multiples, topographic variations), TPAO performed the following processing steps to the seismic reflection data. An example of the processed data is shown in Figure 15. These processing steps include:

- There is no datum processing, and bulk is zero microseconds (ms)
- Gain correction
- Surface consistent amplitude balancing
- Deconvolution (50 hertz, noise suppression)
- Bandpass filter
- Residual statics
- Residual move-out correction
- Kirchhoff time migration
- The 3D spatial prediction filtering

3.3 Structural Interpretation of the Seismic Data

Seismic reflection interpretation is basically determining the subsurface geological information from the processed field seismic data. A seismic wavelet begins as a pulse of acoustical energy that is produced by some type of source such as dynamite, seismic vibrator, or hammer and this energy moves down from the surface and interacts

with subsurface acoustic impedance contrasts. Then, the energy returns to the surface receivers carrying the geological and geophysical data. This seismic wavelet generally is of minimum phase of frequency and width, and it is returned as a zero- phase wavelet (Brown, 2004; Kern, 2011). The reflected seismic wavelet carries the geologic information, therefore, is the most important part of seismic interpretation is to define the known characteristic details of the area's geology and to constrain the results with other geologic and geophysics methods such as well logging and gravity.

Seismic reflection interpretation is an important part of the developing a geophysical study, when geological features and geophysical data are integrated with each other. Seismic reflection interpretation is not only performed using the seismic reflection data to reach a model but it also is integrating geological and other geophysical data as there is non-uniqueness in the models. Thus, geological features should be determined in an integrated way to provide more confident results (Yilmaz, 1987; Kazei et al., 2013). To aid in this, the Petrel™ software package was used mainly to interpret the horizons and faults to create an image on the subsurface. The Petrel™ software is a program which brings different disciplines together and allows us to use them very effective way. It includes seismic data modelling, determine rock physics, and reservoir features.

Horizon Interpretation. In this step, the seismic traces were highlighted and picked to build a seismic model and define the subsurface features (depth to reflectors, locations of faults) in the model. All the seismic slices were both picked on in-line and x-line to improve accuracy and to provide a check the other line picks. All these slices are on the time domain. The horizons were picked from the Osmancik and the Danismen

Formations using the Petrel™ software to find the formation borders on both the x-line and in-line sections (Figure 16).

Also, the check shot data was used in this interpretation step. All the picks were transferred from each line to identify an image on every two slice pair for making a more accurate digitalization of the data. The final picks indicated that there is both a pull-apart basin and an anticlinal structure.

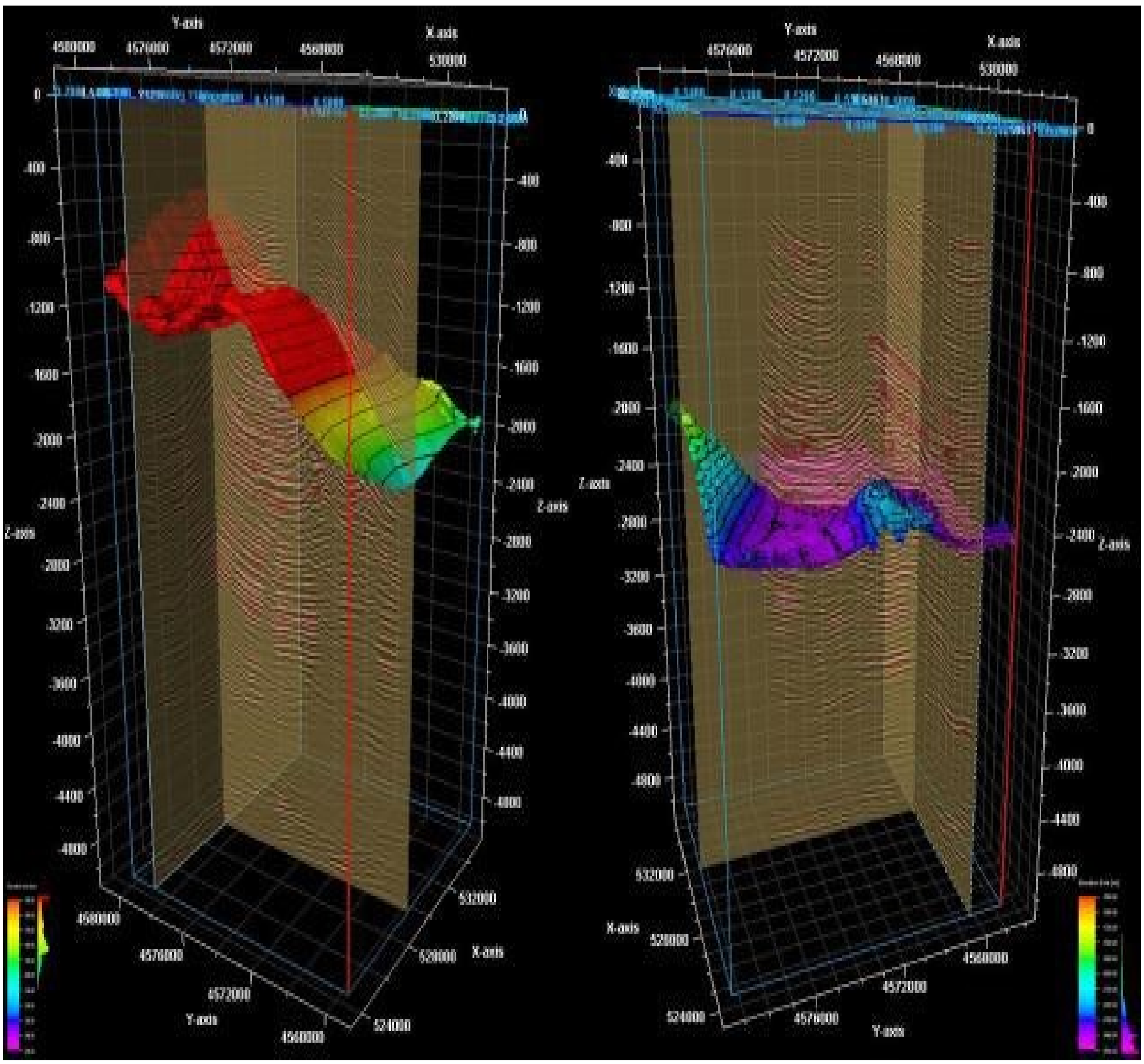

Figure 16. The picked horizons (shown in color) based on the Osmancik and the Danismen Formations as interpreted from the seismic reflection profiles. Colors show the depth in meters. The z-axis is in milliseconds (twt), and the distances are in meters.

A pull-apart basin is structural basin that is created by overlapping strike-slip faults or bending of strike-slip faults, where the result is a down-dropped or rotation of a block (Caldwell, 1997). In the Thrace basin normal faults are the most common type of fault but on the northeastern side of the basin there are strike-slip fault systems caused mainly by the NAFs. These strike slip faults caused pull-apart basins, including the one shown in Figure 17. Pull-apart basins are rare on the south side of the Thrace basis because there are numerous fracture systems caused by the Miocene tectonism that broke up the basins.

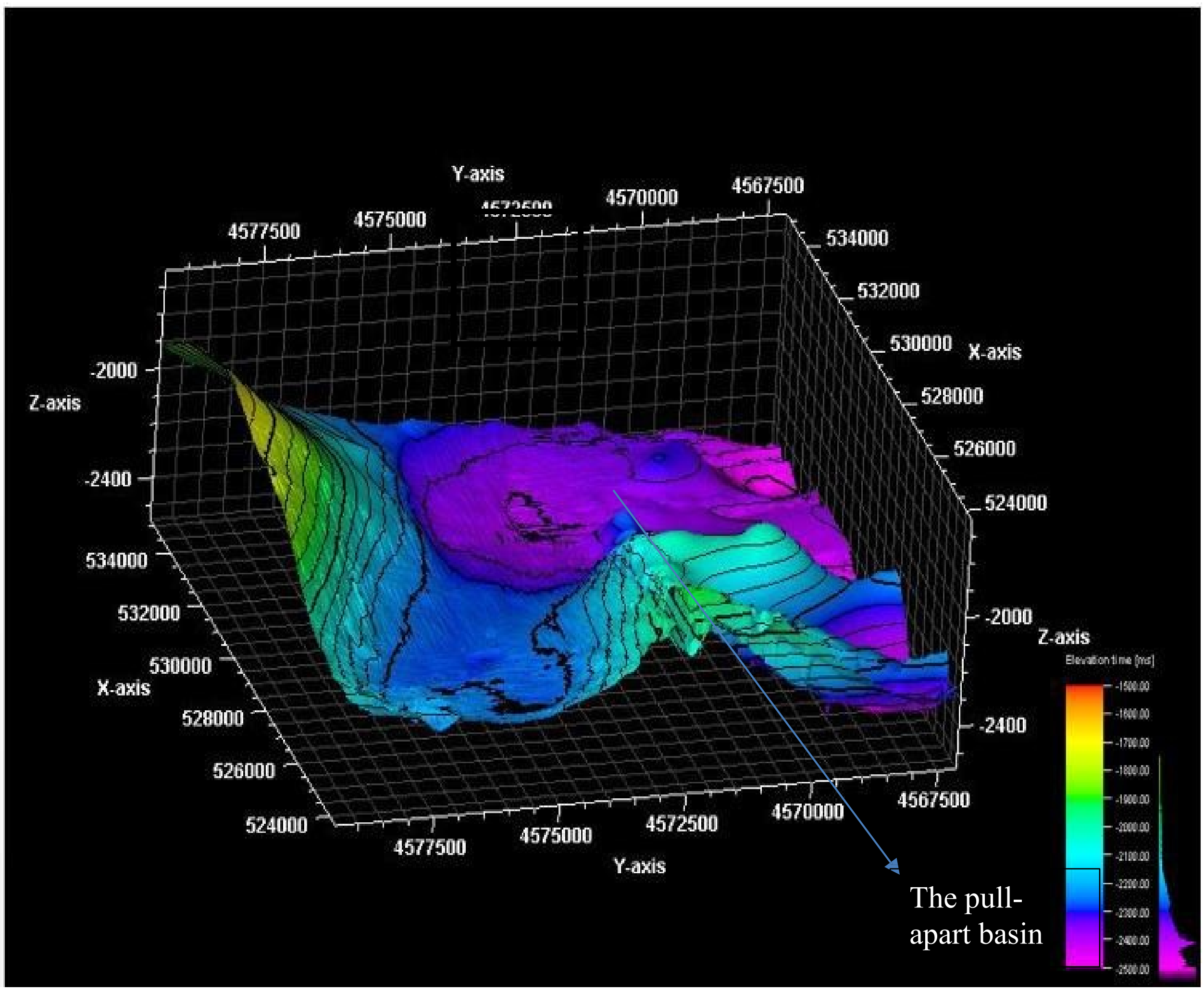

Figure 17. Pull-apart basin in the Thrace basin based on the interpretation of seismic reflection data. Colors show the depth in meters. The z-axis is in milliseconds (twt), and the distances are in meters.

The Thrace basin that was filled with sediments by Miocene time and was folded on the north, and these folds include a series of anticlines and synclines (Bozkurt, 2003). The digitalized seismic data were picked to demonstrate the geologic structure of the basin including an anticlinal structure (Figure 18). These anticlinal structures can be traps where hydrocarbon accumulates, and the study area seemed to not have been affected highly by Miocene tectonism. Thus, it is possible to find hydrocarbon accumulation this type of anticlinal trap.

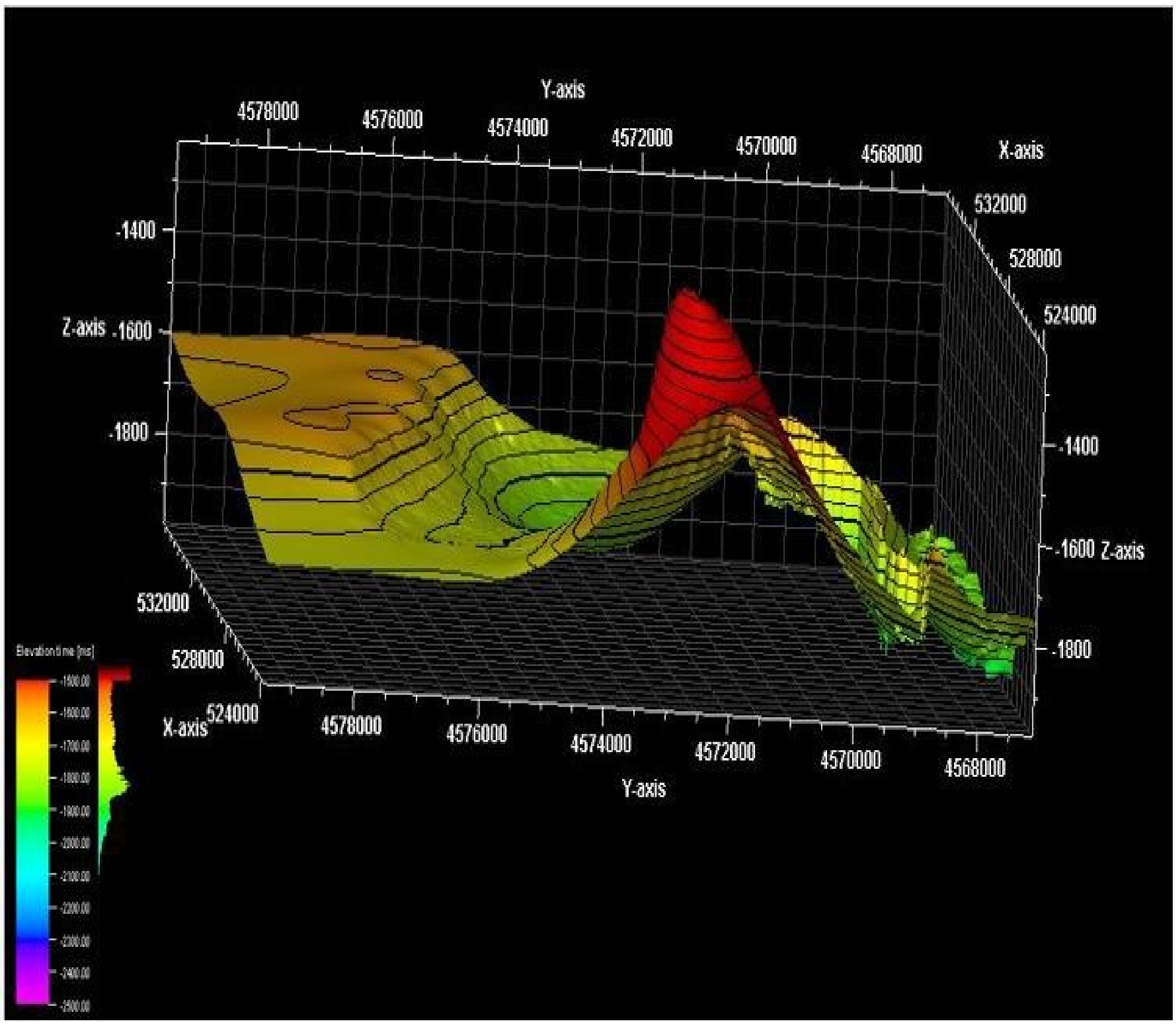

Figure 18. An anticlinal structure based on the interpretation of the seismic reflection data. Colors show the depth in meters. The z-axis is in milliseconds (twt), and the distances are in meters.

Fault Interpretation. After digitalizing the seismic horizons, all shown faults were picked to show the main fault system on every ten slices of the seismic reflection data. Fault picks were represented different color to distinguish them from seismic horizon picks (Figure 19). As previously above, the normal fault systems include the Kirklareli, Luleburgaz, and Babaeski fault zones that were highly affected by the NAFs (Figure 19).

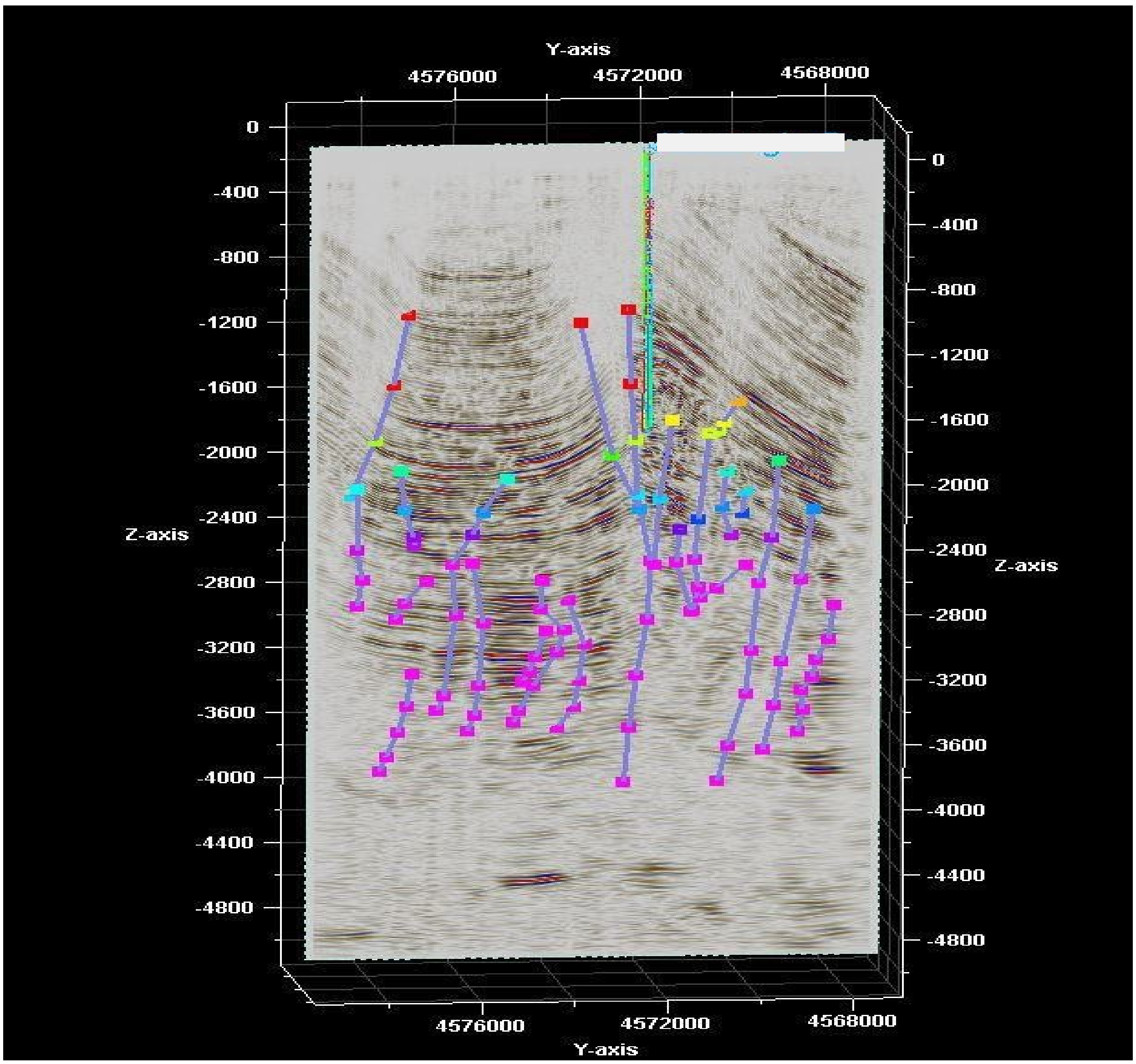

Figure 19. Interpreted normal and strike-slip faults superimposed on the seismic reflection data and Well 2 well within the study area. The z-axis is in milliseconds (twt), and the distances are in meters. Also shown is the well Well 2.

The normal faults were bent, and these faults became a strike-slip fault system on the northeast side of the Thrace basin (Bozkurt, 2003). The fault model was created in on this model and supported by the interpretation of the seismic data to demonstrate the positive flower structure that showed there were strike-slip faults within the study area (Figure 20). Positive flower structures that are also called “Palm-tree” or “Push-up” are formed as raising via bending and folding by wrench (strike-slip) type faults (Pace et al., 2012).

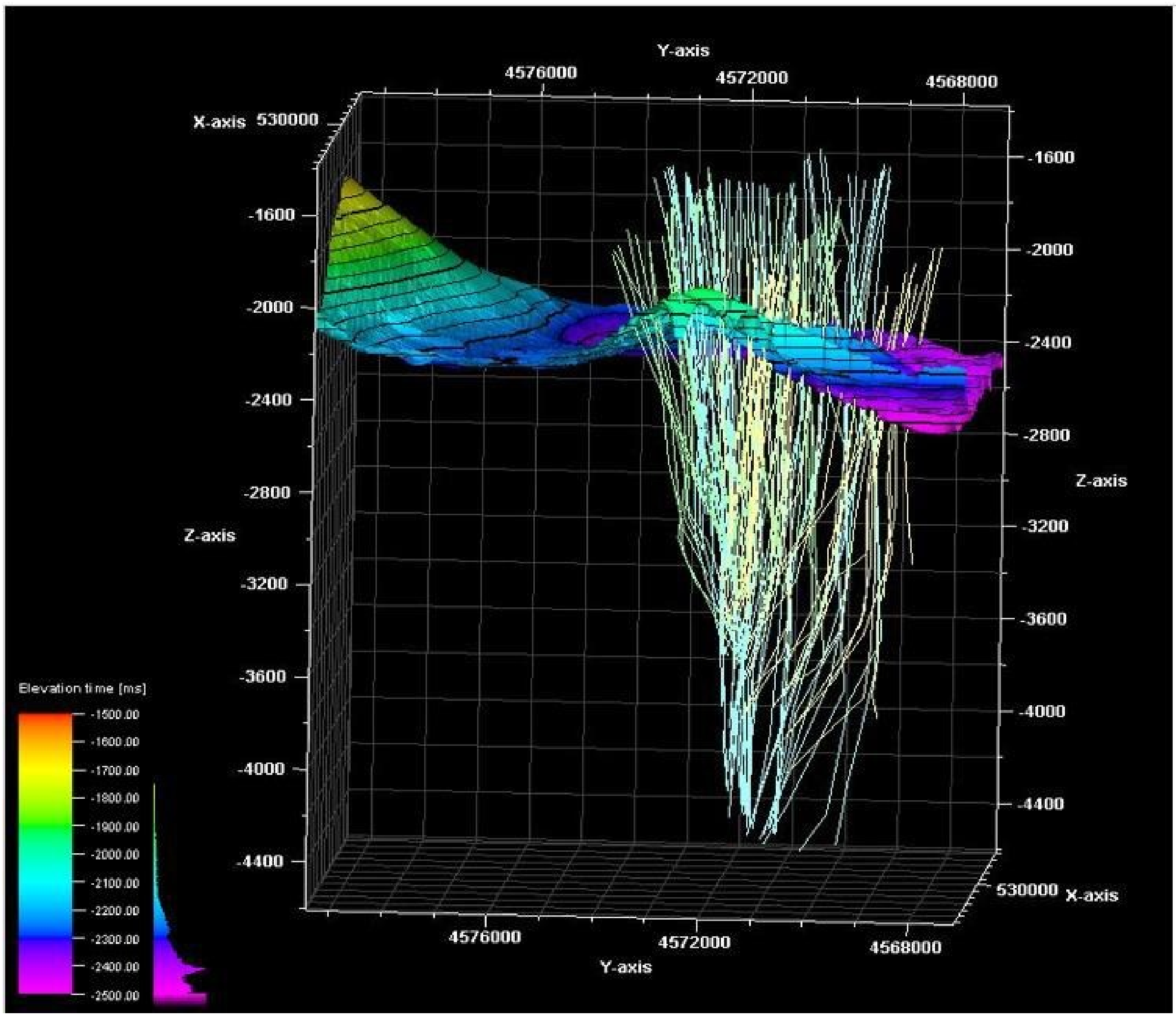

Figure 20. The modeled faults and positive flower structure within the study area. The colors on the horizon show depth, and two different colors were chosen to show the part of flower structure faults for yellow (right) and blue (left). Colors show the variations in depth in meters. The z-axis is in milliseconds (twt), and the distances are in meters.

CHAPTER 4

4.1 Well Logging Fundamentals

Well logs are the recordings of geophysical parameters (e.g. velocity, density, and radioactivity) using a variety of instruments passing through the well from bottom to the top. The recorded value is plotted as a function of depth of the borehole. For the study area, there are three well logs which are Well 1, Well 2, and Well 3 (Figure 21). On this part, the Hampson-Russel^{TM} and Petrel^{TM} software used to interpret and plot well logs data for enhancing visual results' diversity because both of the two softwares have distinct advantages over each other.

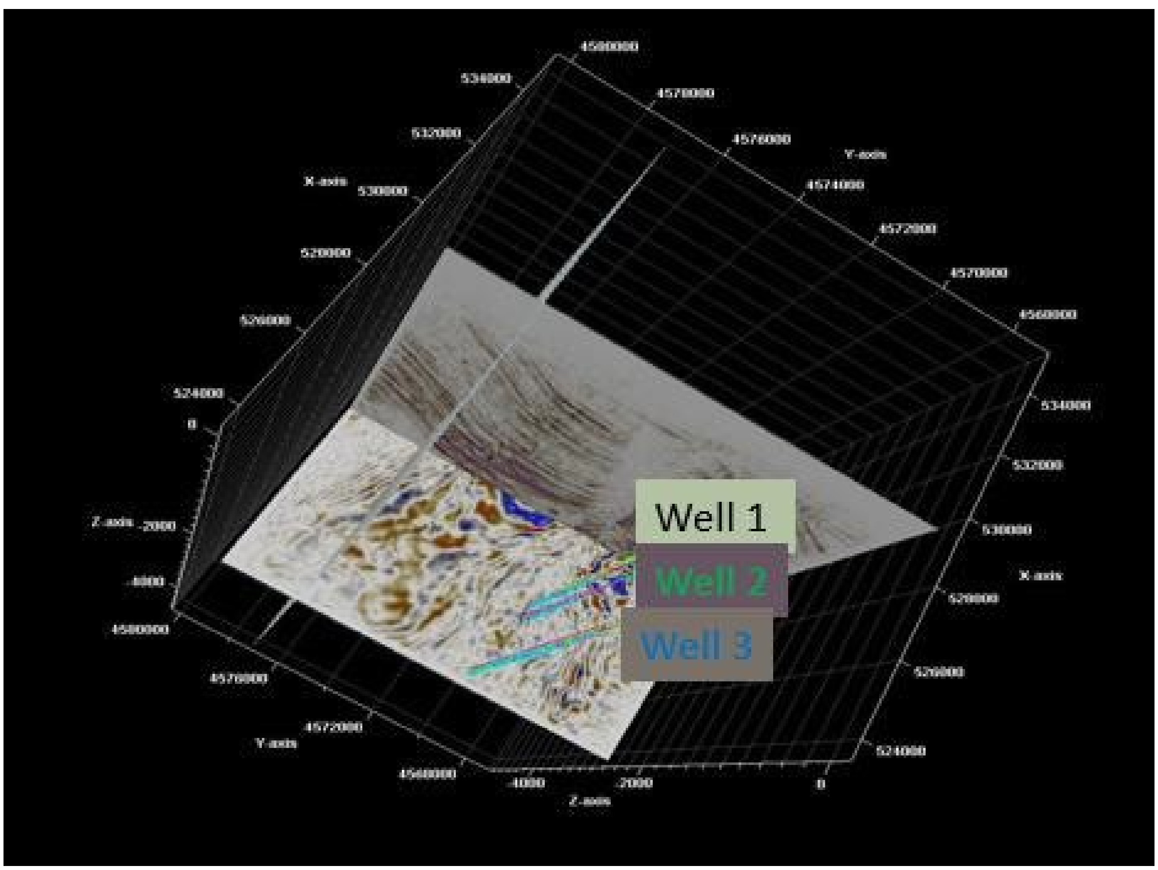

Figure 21. The three wells (Well 1, 2, and 3) superimposed on a seismic reflection data. The z-axis spaces on the seismic cube are in milliseconds (twt).

The general features of recorded wells showed on the Table 1. According to the TPAO’s check shot data, two formations that are the Danismen and Osmancik were identified down to the maximum depth (2,875.0 m), so just these formations were analyzed on this study (Table 1).

Table 1. Well logs general features in the study. (MD = Measured depth, SSTVD = Sub-sea true vertical depth).

Well Name (UWI)	Start Depth	Stop Depth	Danismen MD	Danismen SSTVD	Osmancik MD	Osmancik SSTVD
Well 1	6.50 m	2,845.20 m	235 m	184 m	1,440 m	1,389 m
Well 2	9.50 m	1,747.44 m	234 m	166 m	1,293 m	1,224 m
Well 3	9.50 m	1,413.50 m	235 m	172 m	1,296 m	1,233 m

The properties measured consist of gamma-ray (GR), resistivity, neutron porosity (NPHI), density (DRHO), spontaneous potential (SP), caliper (CALI), and sonic log (DT). Well 3 has also photo electrical log (PEF) (Table 2). However, The PEF logs do not include measured shear-wave velocity information.

Table 2. Type of logs which were used in the study.

Type of Well	Generalities	Symbol, Abbreviation
Gamma-Ray	Radioactivity measurement	γ , GR
Resistivity	Formation conductivity.	R_{D}, LLD / R_{S}, LLS / R_{XO}, MSFL
Self-Potential	Natural potential differences.	, SP
Porosity and Density Logs	Porosity calculation and preliminary interpretation of hydrocarbon accumulation.	ϕ_n, NPHI / ρ, RHOB/ / ρ, DHO
Sonic Log	Calculation the porosity of formation and density with interval transit time	Δt_p, DT

Gamma-Ray Log (GR). The GR log measures the formation's radioactivity, a value that is usually related to the amount of shale. The GR log is useful in making stratigraphic correlation and to identify specific lithologies. The radioactivity is caused by the decay of uranium, thorium and potassium radioisotopes within mainly potassium-rich minerals, and is mainly used for calculating shale volume. Most rocks have radioactive elements to a certain extent, whereas sediments emit less radioactivity than igneous and metamorphic rocks (Rider, 1991). On the GR log, shale generates high radioactive values while sandstones and carbonates generally include less radioactive material.

Self Potential Log (SP). The SP method measures the natural potential contrasts and/or self potentials that are between the electrodes in a well and at the surface (Rider, 1991). The SP log is also used to determine the shale volume and formation permeability.

Porosity and Density Logs (NPHI, RHOB, DRHO). The RHOB is the total density of the solid matrix including rock's porosity and fluid in the pores of the formation. The RHOB log can be used with the NPHI which is associated with existing of hydrogen on the formation to decide the formation porosity and the nature of the pore fluid. The amount of hydrogen in the pore spaces can be calculated if they are associated with carbon (oil and gas) or oxygen (water) by a neutron porosity log.

The NPHI log is mainly used to measure water and hydrocarbon matter in the formation (Rider, 1991). In well logs investigation, using both the RHOB and the NPHI logs in combination is the best way to detect the hydrocarbon accumulation. If there are higher neutron and lower density, and they touch or cross each other on the one column, it shows the volume of the gas bearing zone and quality of the reservoir (Figure 22; Luthi, 2000). The NPHI and the RHOB logs were used to calculate reservoir zone fatures

and area’s petro-physical features which are volume of shale, water saturation, and porosity.

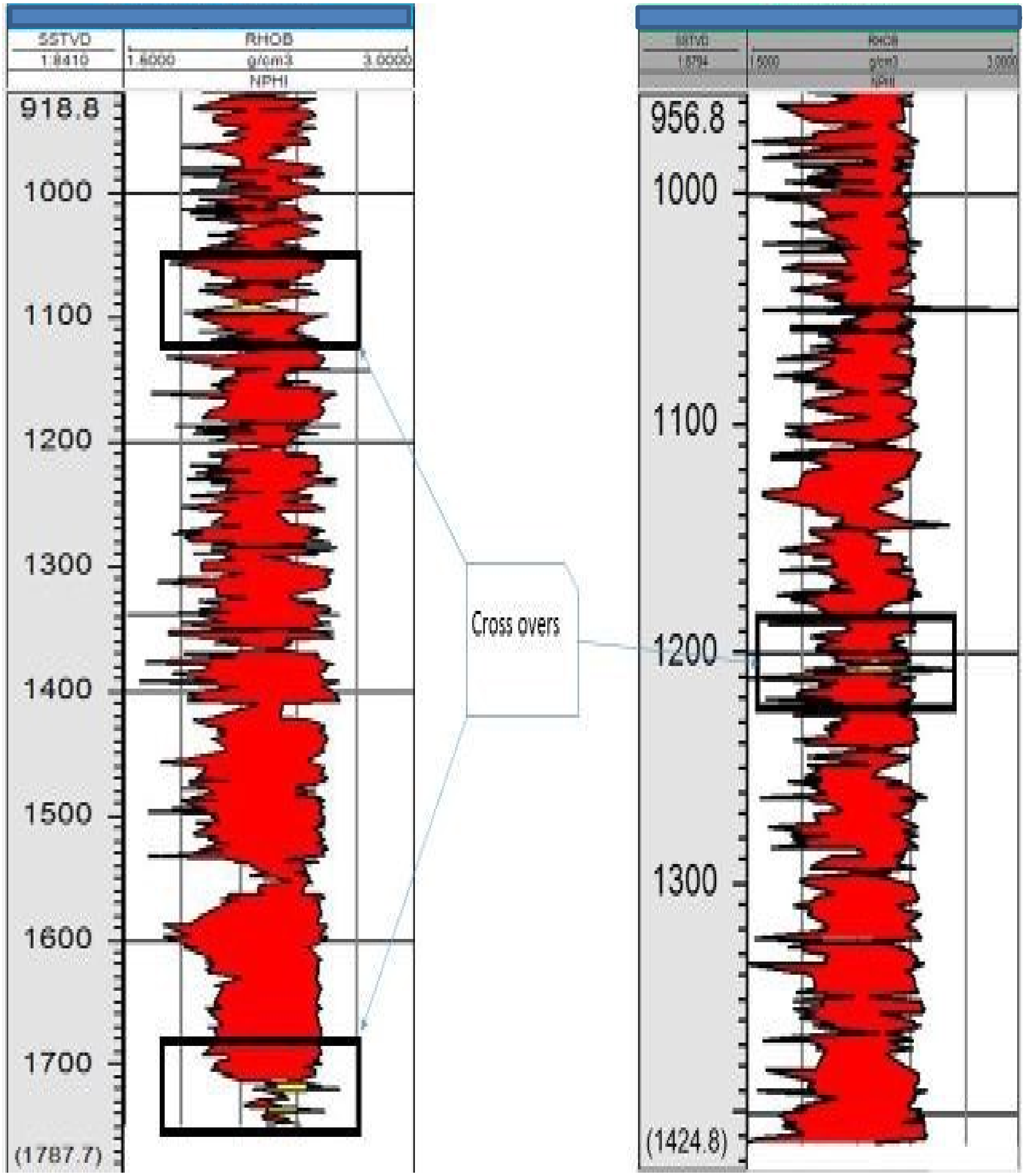

Figure 22. The NPHI and the RHOB well logs crossed over on the border that are for Well 2 between 1,090 and 1,095 and 1,760 and 1,775 meters, for Well 3 between 1.210 and 1,215 meters. The yellow colored areas in the black rectangle that are crossing the RHOB and the NPHI show probable hydrocarbon accumulation areas.

Sonic Log. Sonic log displays the duration of interval transit time (Δt) of the P wave. The sonic log measures the travel time of sound wave to calculate formation's content features which are dependent of the lithology, rock type, and porosity (Rider, 1991). The sonic log can be advantageously utilized in seismic interpretation to find duration of the sound wave velocity, and acoustic impedance log that was made by the TPAO can be created by the sonic log.

The interval transit time is calculated as follows (Rider, 1991):

1 microsecond = 1 x 10^{-6} second

$$\text{Velocity} = \frac{1}{\Delta t * 10^{-6}} \tag{4.1}$$

where delta t is measured on the sonic log.

Resistivity Logs. Resistivity logs measure the formation's electrical resistivity which is its resistance to the electric current. The resistivity log was established mainly to search for hydrocarbon reservoirs. Also, it can be used to determine permeable zones (Rider, 1991; Hearst et al., 2000). There are MSFL (micro spherically focused log), LLS (shallow lateral log), and LLD (deep lateral log) resistivity logs. Within the reservoir zone, all three resistivity logs can show a curve which indicates an abrupt increment of gas zone because hydrocarbons have infinitive resistivity features unlike other fluid. Thus, sudden changes on the log's curve can be easily identified on the resistivity logs.

4.2 Well Log Correlation

In this chapter, the wells' physical features were matched with each other using check shot data to identify formation boundaries and general rock types according to the GR or GR and SP logs curves. A well log correlation is not sufficient to interpret

geologic subsurface features but it is used mainly supporting seismic reflection interpretation results. Well log correlation is mainly used to find hydrocarbon accumulation but it is also practical for mining and hydrogeology. There are a number of different types of correlation methods, and the litho-stratigraphic correlation method that is mainly based on the GR log or combination of the GR and the SP log (Luthi, 2000). Both methods were used in this part of the study.

In the litho-stratigraphic correlation method, the GR log or a combination of GR and SP logs were correlated connecting similar part of the all three logs data to define the lithologic features of a region and the boundaries of the formations because these well log tools include mainly lithologic information. According to the idea of the well correlation, shale rocks that are middle Eocene age are on the top of the Danismen Formation, and shale has low GR values (Figure 23). There are shale and sandstone present in the middle of the Danismen Formation, and the Osmancik Formation has more sandstones and less shale.

4.3 Reservoir Petrophysical Features

In this part of study, petro-physical features relevant to oil and gas production, which include physical and chemical features of rocks and interaction of fluids with the formation, were calculated. These features include water saturation (Sw), Porosity (Ø), and volume of shale (Vsh). These values were calculated to show the extent of the reservoir zone in accordance with the seismic reflection study (Figure 24).

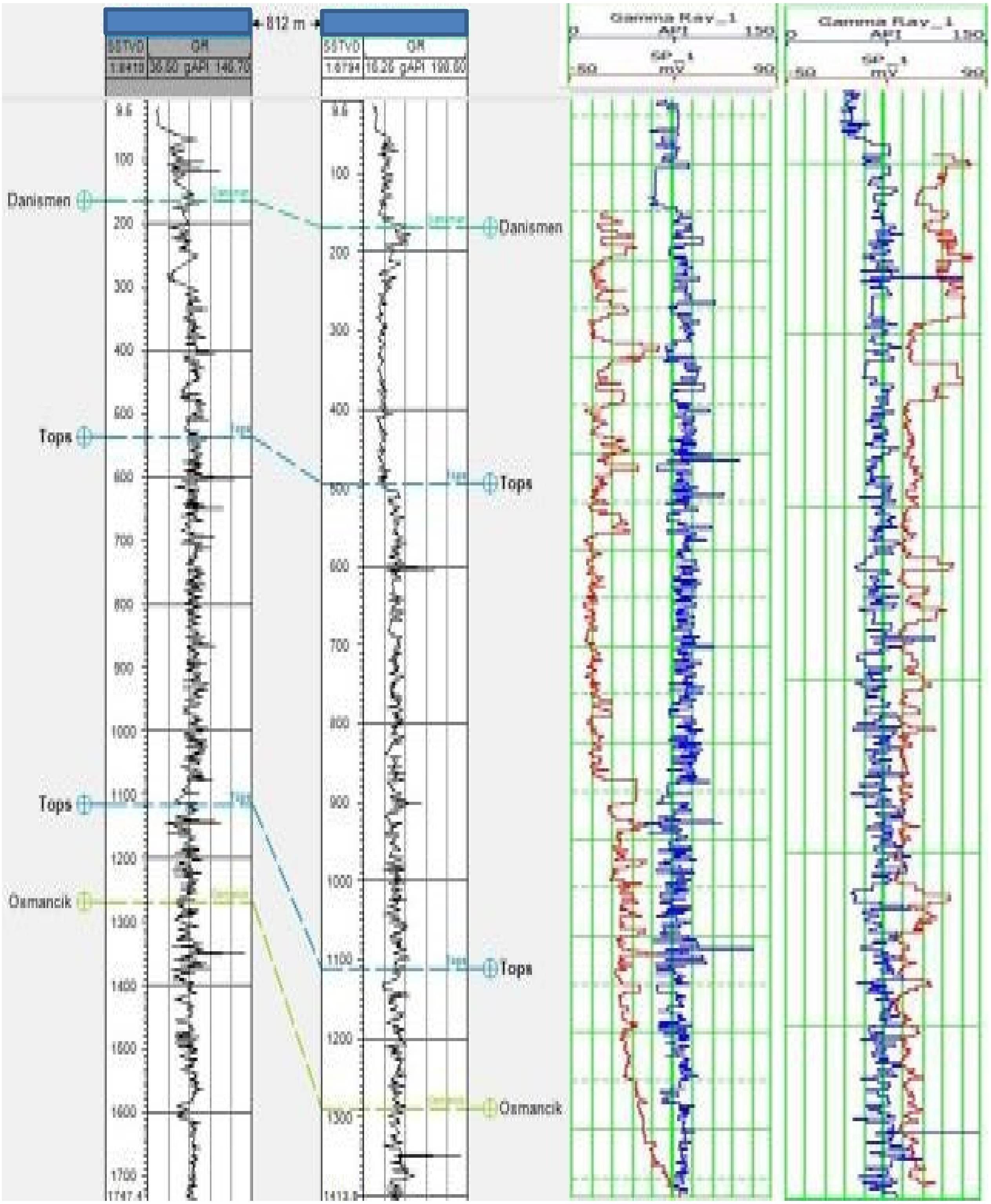

Figure 23. The Well 2 and 3 wells correlation in the study area using the just GR (left), and GR and SP logs (right). Tops on the figures show the changing of rock types from shaly sand to sandstones (less shaly) (left). The Osmancik Formation has mainly sandstone and less shale than the Danismen Formation. The blue line is the GR log and red line the SP log (right).

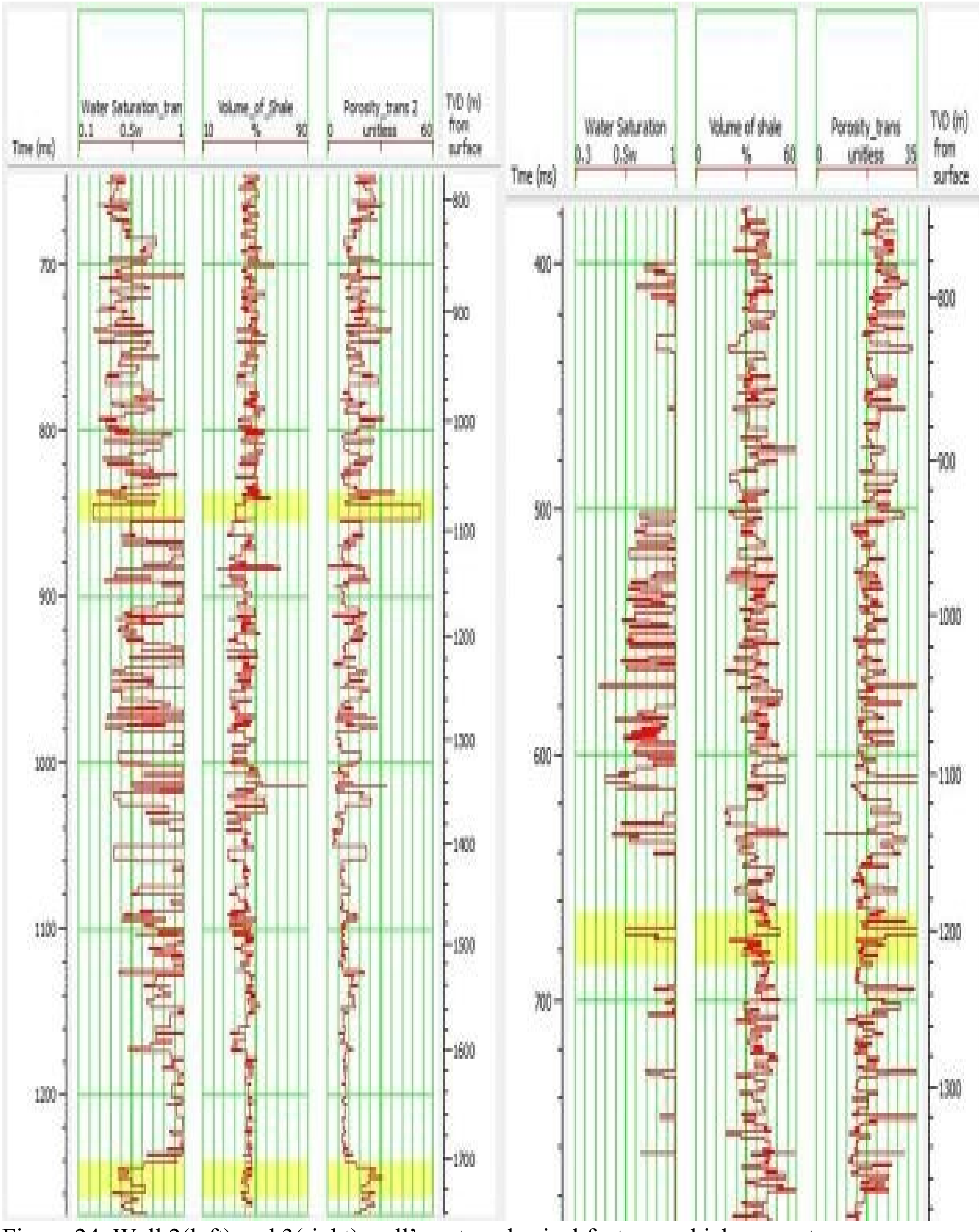

Figure 24. Well 2(left) and 3(right) well's petro-physical features which are water saturation (Sw), volume of shale (Vsh), and porosity (∅). The yellow colored lines show probable hydrocarbon reservoirs.

Volume of Shale (Vsh). One of the first step towards the characterization of the petroleum reservoir zone is the calculation of the volume of shale using the gamma ray log. This step does not only calculate the shale volume but it also helps determining the amount of the water saturation. Shale can hold water within a formation so the water saturation goes up. Also, a formation which has high shale volume shows low permeability (Hearst et al., 2000). There are many formulas for the shale volume calculation as shown below (Figure 25). After these formulas were calculated and plotted, the formula proposed by Larionov (1969) for older rocks was selected for this study. The formulas are:

for older rocks Larionov (1969):

$$V_{sh} = 0.033*(2^{(2*IGR)-1}) \tag{4.2}$$

for tertiary rocks Larionov (1969):

$$V_{sh} = 0.083*(2^{(3.7*IGR)-1}) \tag{4.3}$$

Stieber (1970):

$$V_{sh} = \frac{IGR}{3 - 2 * IGR} \tag{4.4}$$

To calculate volume of shale (Vsh), it is required to first find the Index gamma-ray value (IGR) using the gamma-ray reading and then using the equation:

$$IGR = \frac{GRlog - Grmin}{Grmax - Grmin} \tag{4.5}$$

where IGR is the gamma ray index, Vsh is the shale volume, GR log is the gamma ray reading, GR min is the minimum gamma-ray reading, and GR max is the maximum gamma-ray reading.

	Vsh	Vsh	Vsh	Vsh
IGR	Linear	Stieber	Larionov (1)	Larionov (2)
0.00	0.00	0.00	0.00	0.00
0.05	0.05	0.02	0.01	0.02
0.10	0.10	0.04	0.02	0.05
0.15	0.15	0.06	0.04	0.08
0.20	0.20	0.08	0.06	0.11
0.25	0.25	0.10	0.07	0.14
0.30	0.30	0.13	0.10	0.17
0.35	0.35	0.15	0.12	0.21
0.40	0.40	0.18	0.15	0.24
0.45	0.45	0.21	0.18	0.29
0.50	0.50	0.25	0.22	0.33
0.55	0.55	0.29	0.26	0.38
0.60	0.60	0.33	0.30	0.43
0.65	0.65	0.38	0.36	0.48
0.70	0.70	0.44	0.42	0.54
0.75	0.75	0.50	0.49	0.60
0.80	0.80	0.57	0.56	0.67
0.85	0.85	0.65	0.65	0.74
0.90	0.90	0.75	0.75	0.82
0.95	0.95	0.86	0.87	0.90
1.00	1.00	1.00	1.00	0.99

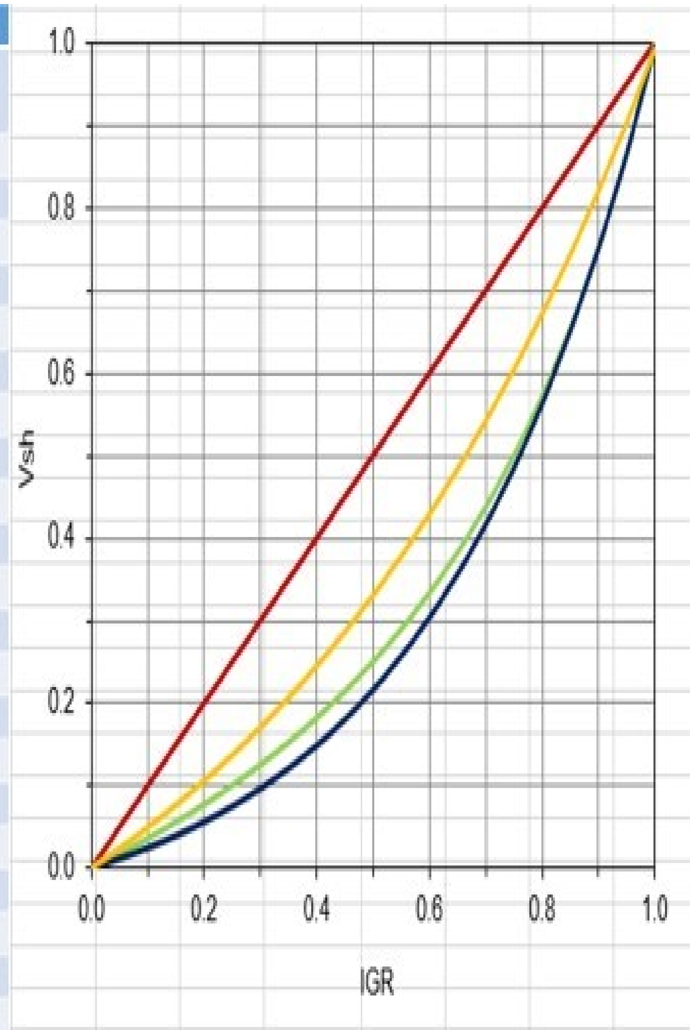

Figure 25. Volume of shale calculations according to the formulas listed in the text which include equation 4.5 (red), equation 4.4 (green), equation 4.3 (blue), and equation 4.2 (yellow).

Water Saturation (Sw). Water saturation is described as the ratio of water volume to pore volume on the formation and can be calculated using electrical resistivity log and porosity of the formation.

$$Sw = \left(\frac{a}{\emptyset^m} * \frac{R_w}{R_t}\right)^{\frac{1}{n}} \tag{4.6}$$

where Sw is water saturation, Ø is Porosity, Rw is formation water resistivity, Rt is true resistivity, a, m, and n are Archie's parameters (Archie, 1942). Archie's parameters for

sandstone are: a= 0.62, m= 2.15, the n value can be arranged from 1.6 to 2.2, it is required to calculate formation porosity.

Porosity (Ø). Porosity can be described the ratio of the pores in the rocks to entire rock's volume. Actually, there is no log to measure porosity but it can be calculated using alternative methods from logs (Hearst et al., 2000). In this study, porosity was calculated using density and neutron logs.

$$\emptyset d = \frac{\rho matrix - \rho log}{- \rho fluid} \tag{4.7}$$

where Ød is the density-derived porosity, ρmatrix is the matrix density, ρfluid is the fluid density (the value of ρfluid and ρmatrix depend on the lithology), and ρlog is the density log reading. On this study, ρmatrix is 2.644 g/cc for sandstone, and ρfluid is 1.088.

For gas reservoir:

$$\emptyset = \sqrt{\frac{(\emptyset d)^2 + (\emptyset n)^2}{2}} \tag{4.8}$$

where Ø is the porosity, Øn is the neutron porosity that is from neutron log, and Ød is the density porosity.

4.4 Well to Seismic Tie

A well to seismic tie which is also called well tie is a method of correlating seismic reflection data to well log data in order to identify the picking horizons in seismic reflection data accurately. On this method, the first step is digitalizing the acoustic impedance log that is defined as a depth from density and sonic log. Then, the acoustic impedance log can be used to calculate the reflection coefficient and a wavelet that include same the frequency respond as seismic reflection data which is defined as a time.

In the last step, the reflection series is produced from the wavelet convolving with the acoustic impedance, and the seismic series are correlated with the original seismic reflection data (Figures 26 and 27). Moreover, this step is necessary to improve the trustworthiness of seismic data that has lithologic information distant from well logs data (White and Simm, 2003). Before creating a synthetic seismogram, the seismic reflection data was prepared for more accurate data processing; the techniques include zero offset data, noise free seismic, and preserved true amplitudes.

The parameters of the seismic well tie study are:

- Phase rotation: 0 degree
- Time shift: 1 msec.
- Synthetic: Zero offset synthetic
- Wavelet length: 200 msec.

4.5 Well Log Interpretation

According to the study and interpretation of the Well 2 well, the reservoir zone which identified as the shaly sand zone as a shaly sandwich was determined at the depth interval of 1,760 – 1,775 m using mainly GR and other logs, including RHOB, DRHO, and SP (Figure 28). The yellow-colored area on the image of the Well 2 well provides evidence for hydrocarbon accumulation because the reservoir zone has mainly low porosities, which in turn depends on which type of rocks it is.

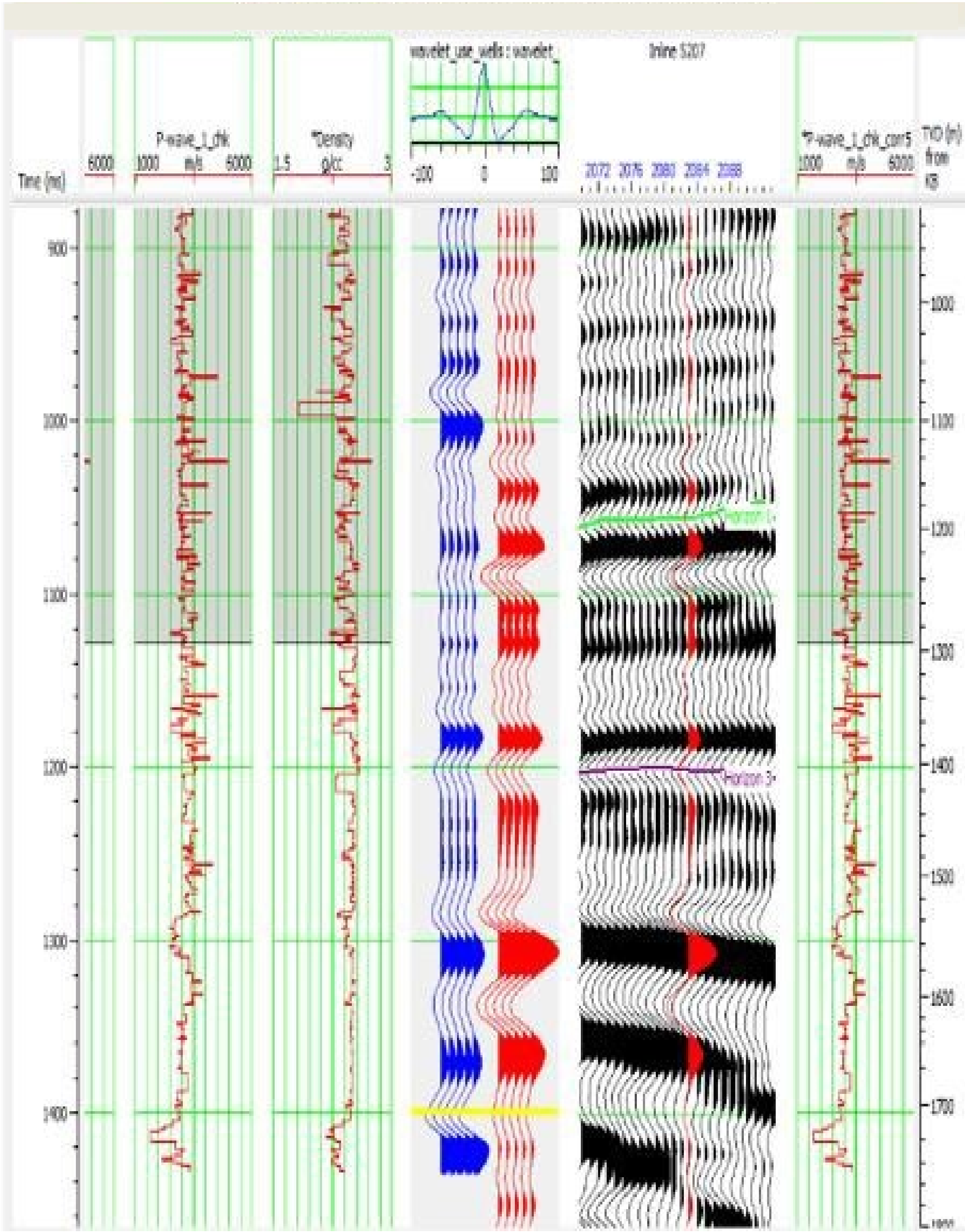

Figure 26. An example of well to seismic tie in calculating a synthetic seismogram for the Well 2 well. Purple and green line shows the picked horizon on the inline panel. Far left panels are the P-wave velocity and density logs, and the correlation with the P-wave is on the right. Real traces are represented as red traces, and synthetic traces which are produced by extracted wavelet from well logs are represented as a blue traces on the middle panel (Correlation between real and synthetic traces is 73.9 %).

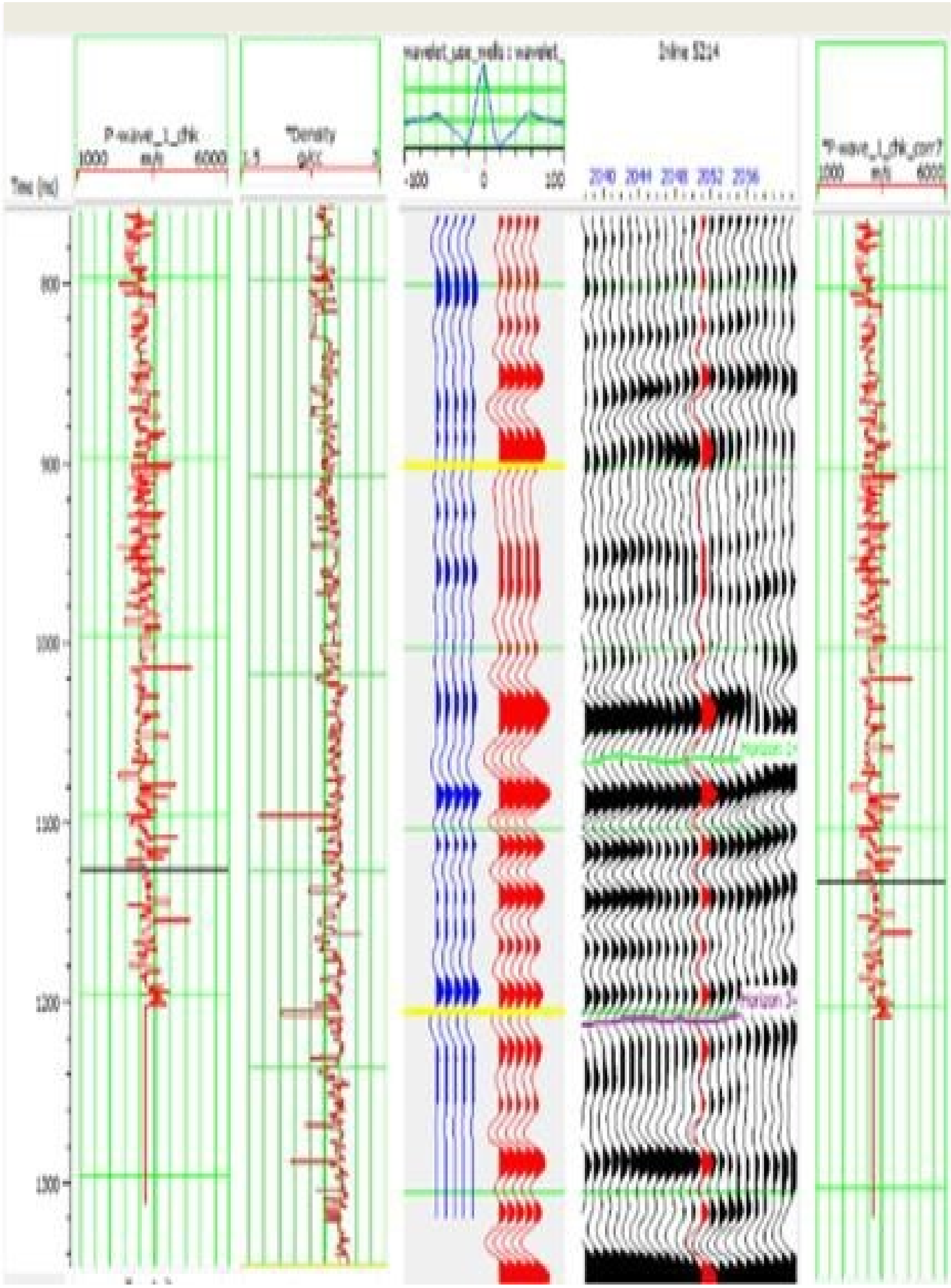

Figure 27. An example of well to seismic tie calculating a synthetic seismogram for the Well 3 well. Purple and green line shows the picked horizon on the inline panel. Far left panels are the P-wave velocity and density logs, and the correlation P-wave is on the right. Real traces are represented as red traces, and synthetic traces which are produced by extracted wavelet from well logs are represented as a blue traces on the middle panel (Correlation between real and synthetic traces is 69.7 %).

Also, the calculated petrophysical features of the well support this area being a reservoir zone. To delineate the gas bearing zone, other logs (gamma-ray, density (RHOB), and resistivity (LLS, LLD)) can be applied to the well log interpretation. If the porosity (NPHI) log is low, density log (RHOB) is high, and GR log also shows decreasing trend at the same time, there is a possibility of hydrocarbon accumulations on the field (Schlumberger, 1994). Thus, the defined yellow-colored area might host a hydrocarbon accumulation.

For Well 3 well, the reservoir zone can be found at about 1,200 meters depth (Figure 29). The well log curves are similar with the Well 2 but the reservoir zone that is yellow colored is not as significant as it was in the other well. Thus, there is lower percentage possibility that the Well 3 log has as much hyrocarbon accumulation as the Well 2 log. The tectonic feaures of the area might have caused this difference, especialy the presence of flower structure.

According to the reservoir petrophysical features for the Well 2 and 3 wells, the volume of shale values which were calculated with the GR log are from 6 to 24 %, and it's averagely 15% using equations 4.2, 4.3, 4.4, 4.5, and 4.6. Also, the porosity was calculated as an average 20% using equations 4.8 and 4.9. The cross plot which was used NPHI log and Vp/Vs rate was plotted for rock petro-physical features of rocks with the Hampson Russell™ software (Figure 30). The reservoir petro-physical features are good indicators of hydrocarbon accumulation, especially the gas bearing zone, which has low water saturation and high porosity values (Figure 24).

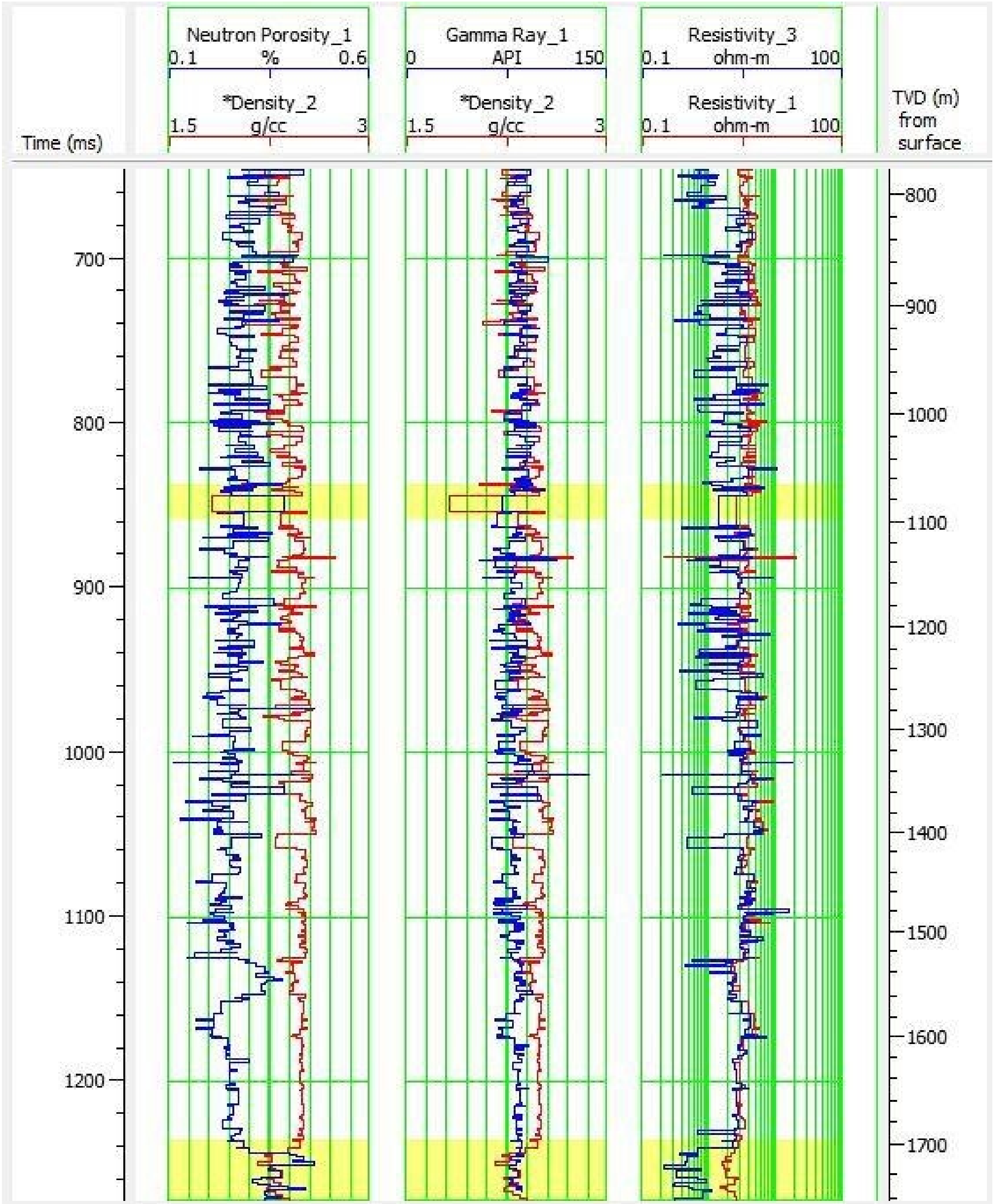

Figure 28. The reservoir zones that are colored (yellow) can be identified to contain hydrocarbons in Well 2. (Neutron Porosity = NPHI, Density_2 = RHOB, Resistivity 1 and 3 = MSFL, LLS)

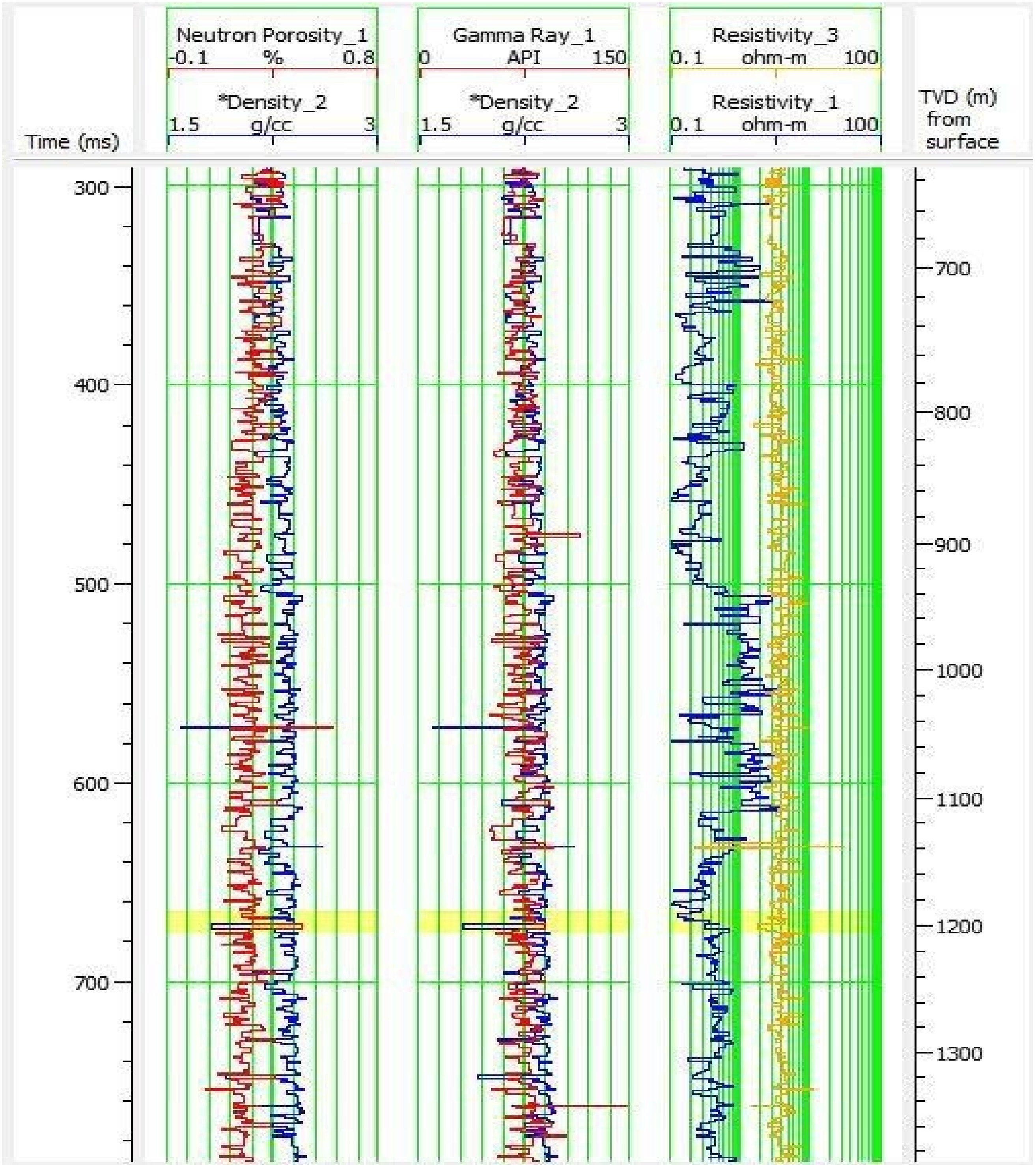

Figure 29. The reservoir zone that is between 1,190 and 1,200 meters on the Well 3 well is shown in yellow. (Neutron Porosity = NPHI, Density_2 = RHOB, Resistivity 1 and 3 = MSFL, LLS)

The compressional wave is susceptible to the fluid type, and its ratio to shear wave velocity which was created in the study, Vp /Vs, can be also used to identify the fluid type. Generally, the compressional wave velocity goes down and shear wave velocity rises with the increment of hydrocarbon saturation. The rock density decreases when the pore spaces are filled by water with low density gas so the compression is increased by water filling that include huge bulk modulus by gas in the pores. Thus, Vp/Vs ratio trends to go down with water filling with gas (Hamada, 2004; Jain, 2012).

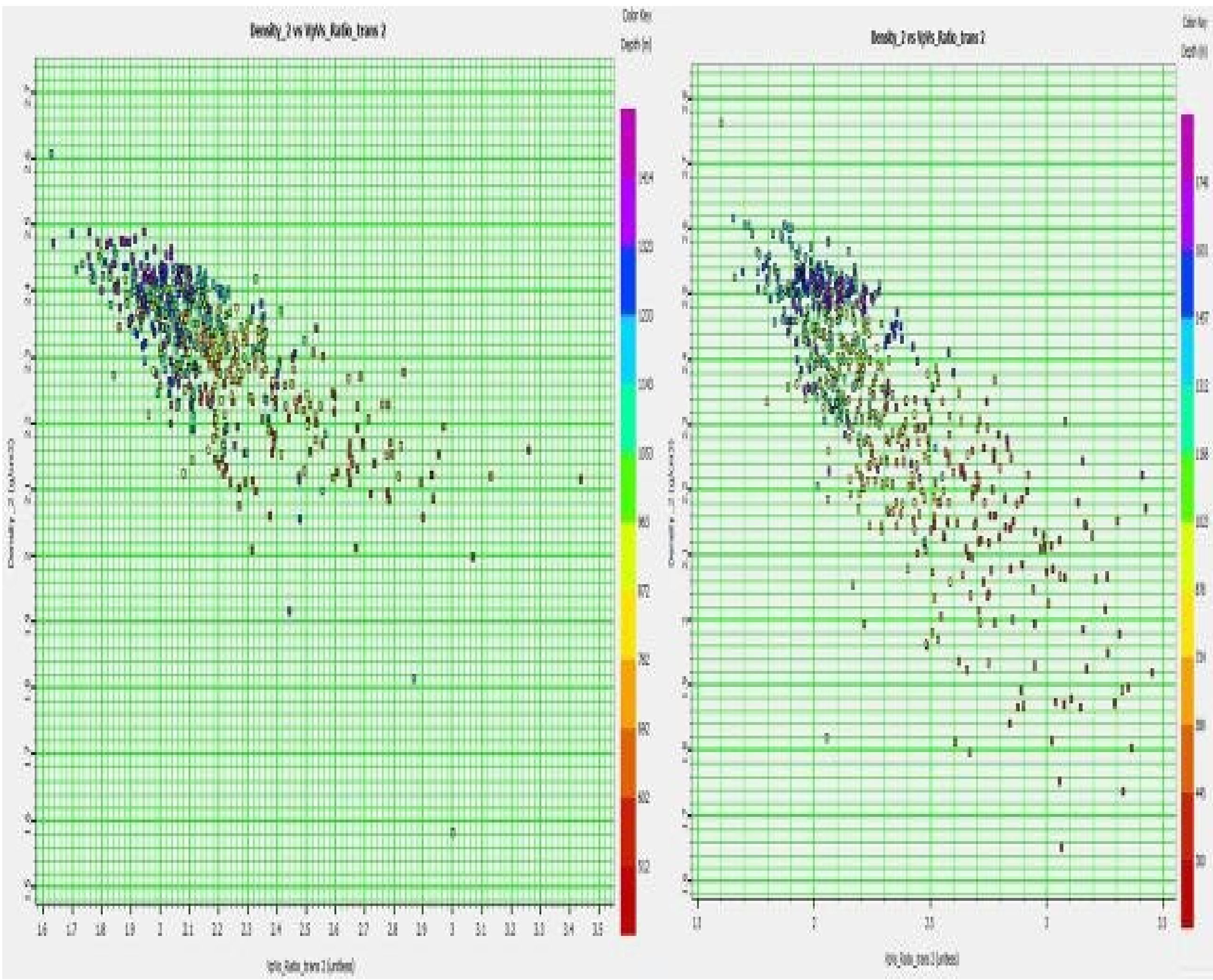

Figure 30. The Vp/Vs – Density cross for the Well 2(left) and Well 3(right) wells. The prediction of density is a major goal in petroleum exploration. Therefore, the relationship between velocities (Vp and Vs) and rock density were plotted.

CHAPTER 5

5.1 Gravity Method

The application of gravity method is mainly used to interpret the location, shape and depth of subsurface density variations. It can be used to search for minerals, geothermal activity, and structures related to hydrocarbon accumulations. Also, it can be the primary or secondary exploration method when searching for minerals, geothermal, and hydrocarbon field using density differences of the subterranean rocks (Rivas, 2009, Demir et al., 2012).

In the gravity method, gravity anomalies are calculated using Newton laws which are universal law of gravitation and second law of motion. The universal law of gravitation is:

$$F = \frac{G * M * m}{R^2} \tag{5.1}$$

The second law of motion is:

$$F = m * g \tag{5.2}$$

These formulas are combined to find relationship between acceleration and mass of the Earth.

$$g = \frac{G * M}{R^2} \tag{5.3}$$

where, F is force, G is gravitational constant that is 6.67 x 10^{-11} $Nm^2 kg^{-2}$, M is mass of the earth, m is mass, R is distance between masses, and g is acceleration (Sheriff, 1994).

5.2 Gravity Data Interpretation

A Bouguer gravity anomaly map is based on contrasts of the gravitational accelerations that is generated by the subsurface density variations (Bonvalot, 2012). Figure 31 shows the Bouguer gravity anomalies within Turkey. The major trend of the gravity anomalies are east-west primarily caused by the east-west trending strike-slip tectonic regime. The blue values represent regions of less gravity caused by thicker low density sediments (Ates and Kearney, 1999).

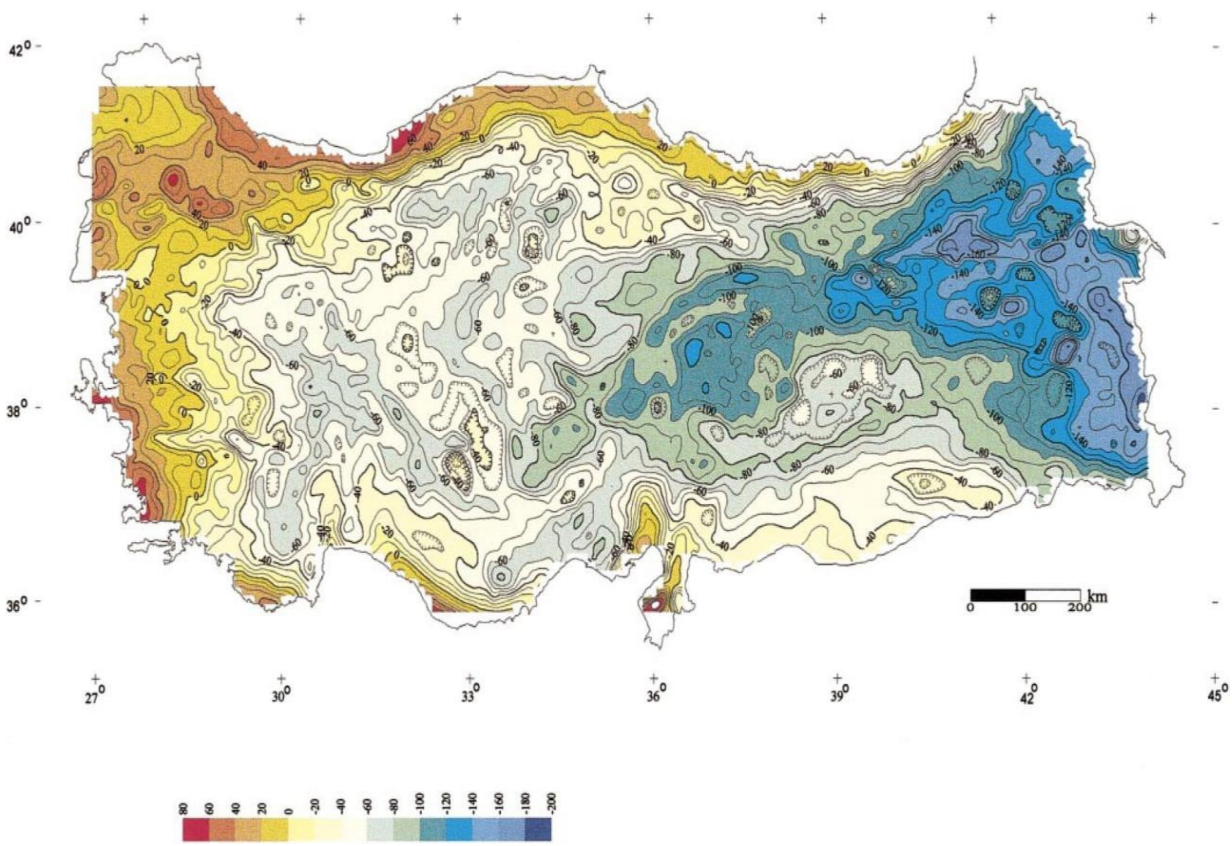

Figure 31. Bouguer gravity anomaly map of Turkey which shows east-west trending anomalies (Ates and Kearney, 1999). Contour interval is 10 mGal.

The validity of applying of the study area's geological information is based on the accuracy of the geoid used in the computing of the free air gravity and the Bouguer anomaly. The gravity data used in this study was obtained from the EGM2008 project (Balmino et al., 2012). The EGM2008 dataset combines a variety of data sources

including satellites land, marine, and airborne sources (Balmino et al., 2012; Pavlis et al., 2012). In this chapter, the Bouguer gravity anomaly data were used to support seismic and well log data in the Thrace basin (Figure 32). The Bouguer gravity anomalies values in the study area range from 105 to 125 mGal, and study area has mainly lower gravity values in comparison to its environment. There is no any significant regional trend to the gravity anomalies within the Thrace basin area which implies that the crust thickness and lower crustal thickness are constant under the basin. However, there are two main trends (Figure 32; anomalies 1 and 2); that can be seen within the Thrace basin.

The residual gravity map (Figure 33) was made by creating a regional gravity anomaly map where the Bouguer gravity anomalies were continued to 2 km above the surface (Jacobsen, 1987). The regional gravity anomaly data was then subtracted from the Bouguer gravity anomaly data to create the residual gravity anomaly map (Figure 33). On the residual gravity anomaly map, the Thrace basin is characterized by a series of gravity minima due to the thick shales and sandstones. The gravity minima mainly trends north-south and is mainly related to the formation of the forearc basin. There are no east-west trending anomalies that correspond to the strike-slip tectonic regime.

The horizontal derivative method determines the magnitude of the gradient in the gravity field and can be used to define the edges of subsurface density variations (Cordell 1979; Blakely and Simpson, 1986; Blakely, 1996). To interpret a horizontal derivative map, one looks for trends of derivative maxima which indicate the lateral boundaries of a dense subsurface body. However, this method is not enough to completely interpret the gravity data. The horizontal derivative results must be compared to other methods

including magnetic and seismic data in conjunction with the geological data to improve the interpretation of the gravity data (Grauch and Cordell, 1987).

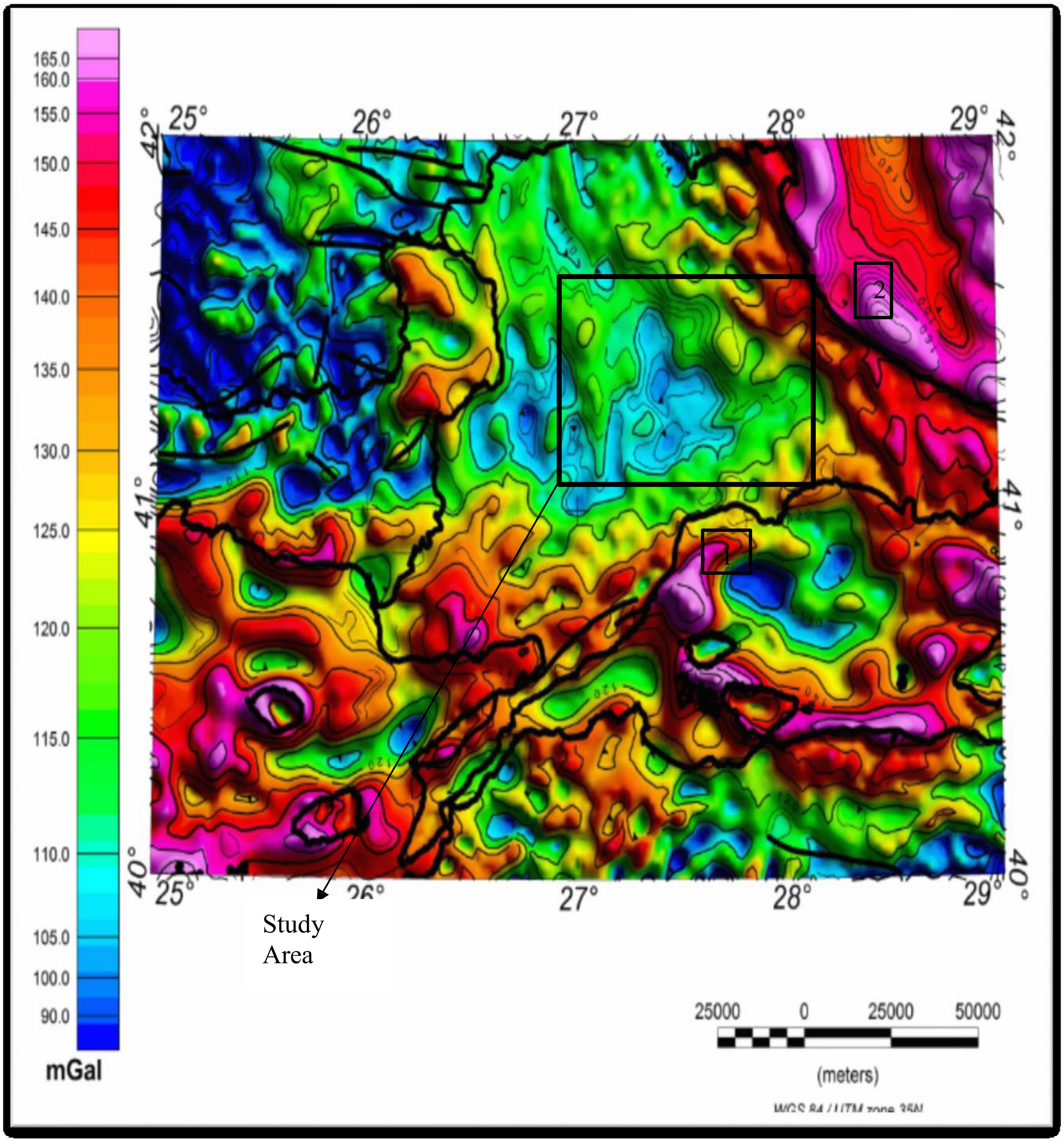

Figure 32. The Bouguer gravity anomaly map of Thrace basin. The contour interval is 5 mGal. These anomalies which are related to region's tectonic history trend east-west (1) and southwest (2).

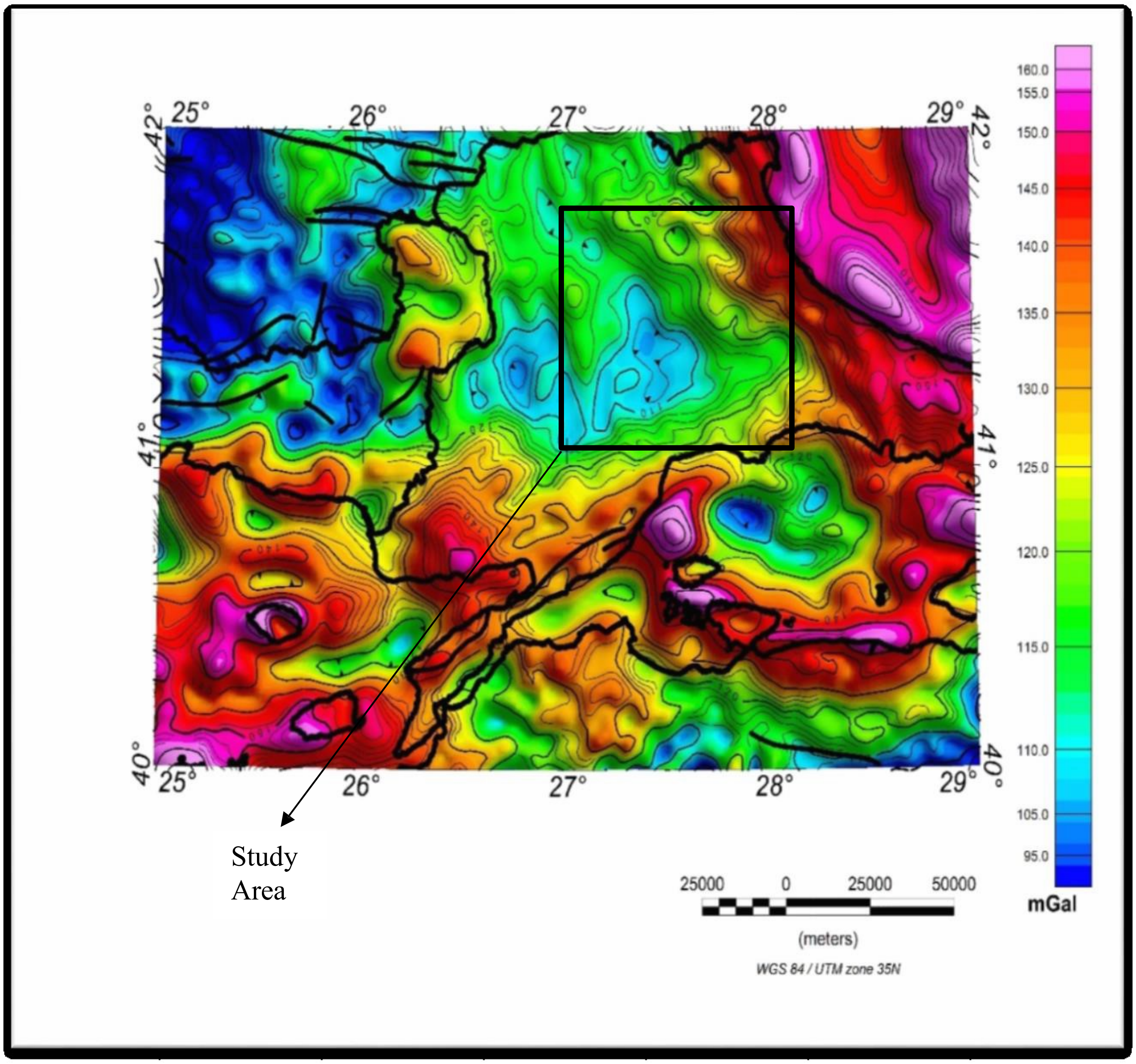

Figure 33. Residual gravity anomaly map of the Thrace basin. Contour interval is 5 mGal.

The horizontal derivative gravity anomaly map (Figure 34) which was created using the residual gravity anomaly data (Figure 33) indicates a series of derivative maxima which trend north-south, northwest-southeast and northeast-southwest. These anomalies indicate a more complex subsurface than suggested by the Bouguer and

residual gravity anomaly maps. These anomalies in general show that the origin of the Thrace basin is complicated, as it has been affected by both compressional and strike-slip tectonics.

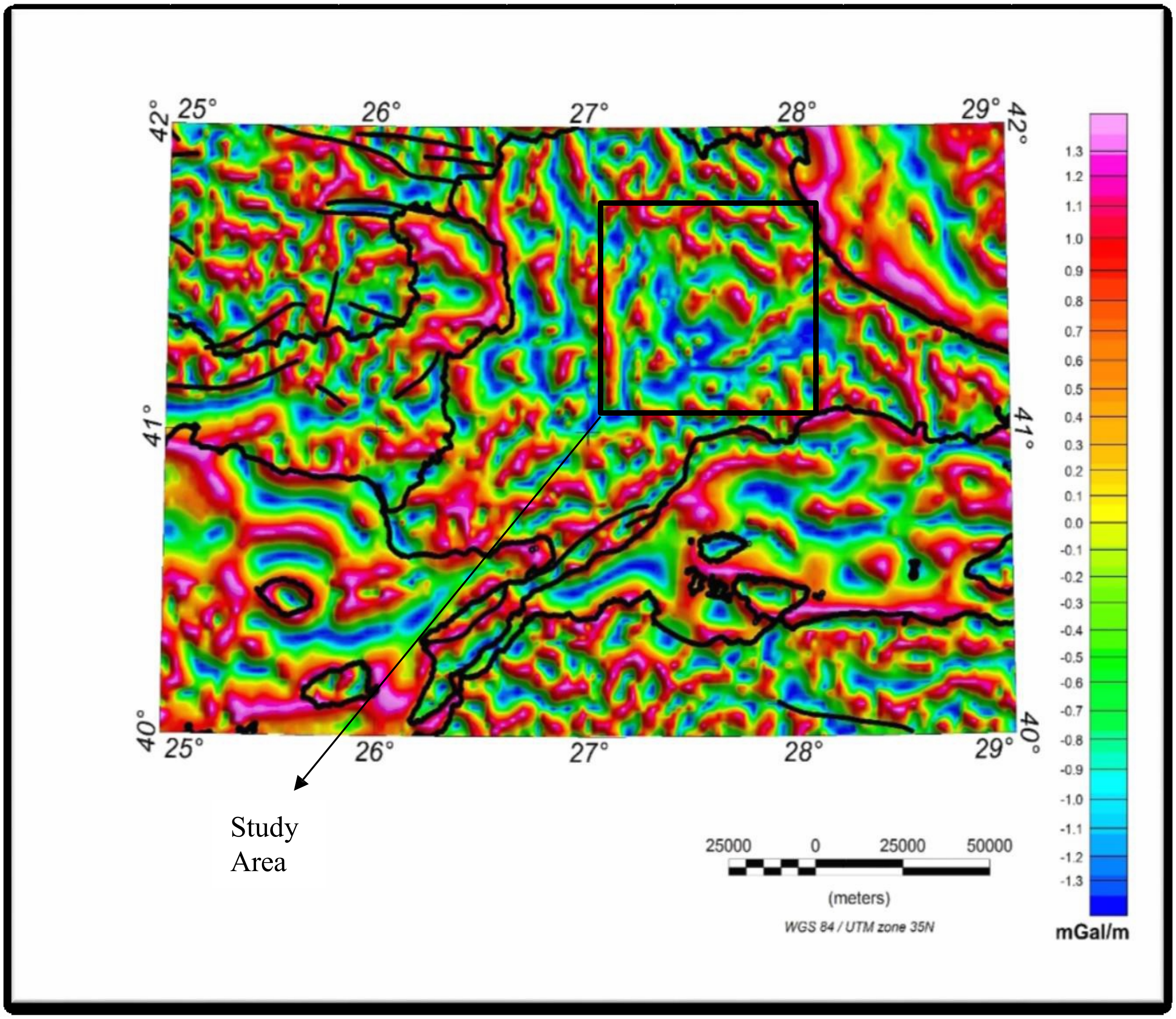

Figure 34. Total horizontal derivative of the residual gravity anomaly map.

CHAPTER 6

6.1 Discussion

This study was undertaken with two main purposes: 1) to define the geological, structural features and petroleum potential of the Thrace basin started forming in the Early Eocene, and 2) to model and interpret seismic reflection, well log, and gravity data compatible with number 1. These purposes were selected to show how the basin has been formed and to determine what the hydrocarbon potential of a part of the Thrace basin. Thus, the study engaged a variety of geophysical methods to evaluate the results from different angles and get more detailed information for the study area within the Thrace basin.

The Thrace basin (Figure 1) was formed by the subduction of the African plate going under the European plate and the escape tectonics caused by the collision of the Anatolian and Arabian plates (Turgut et al., 1983; Coskun, 1996). These tectonic activities formed a variety of structures including horsts and grabens (pull apart basins) along the north side of the basin by the NAFs which has mainly strike slip motions. These structures include the pull-apart basin imaged by the seismic reflection data (Figure 17), where flower structures confirm that this basin was formed by strike-slip tectonics (Figure 20). This tectonic evolution history is a commonly accepted hypothesis for the Thrace basin (Turgut et al., 1983, 1991; Siyako, 2006; Siyako and Huvaz, 2007; Sen, 2011; Derman, 2014). This mode of basin formation also includes the deposition of several geologic formations which are mainly Oligocene-aged sandstones and shales of the Osmancik and Danismen Formations, and with the Oligocene-aged shale, sandstones

and siltstones of the Mezardere Formation comprise the main units with hydrocarbon potential within the Thrace basin. The well log analysis (Figures 28 and 29) showed that the Osmancik and Danismen Formations have a moderate potential for hydrocarbon production. Schindler (1997) showed that the basin depositional systems include turbiditic, deltaic and fluvial phases, and Siyako and Huvaz (2007) revealed that this sedimentation occurred from the Middle Miocene to Pliocene using fossil records (Figure 8). However, there is a difference of opinion about the kerogen types that comprise hydrocarbon production from the Eocene age shale rocks but the TOC values determined by this study are accepted between 0.01% and 6.3% by Burkan (1992) and Soylu et al. (1992). The TOC values of shales, ranging between 2% and 5% are considered to have a good generation potential by the AAPG. The basin's shale content as determined by this study that is primer hydrocarbon production is however limited for Turkey’s hydrocarbon requirements with conventional method but the new shale gas production technology which utilizes unconventional techniques could be very useful to increase hydrocarbon production (EIA, 2015; TPAO, 2015).

6.2 Conclusion

A geologic and geophysical interpretation study of the Thrace basin in northwestern Turkey, via seismic reflection, well log data, and gravity anomaly maps were analyzed to determine the geologic characteristics and hydrocarbon potential of the basin. The study was concentrated on the northern sections of the Thrace basin, where seismic models were constructed from 3D seismic reflection data and were integrated with well log and gravity data.

The 3D seismic reflection interpretation was able to define the several geologic structures including normal and strike slip faults, anticlines and a pull-apart basin. The anticline and pull-apart basin models contained the shallow Danismen and deeper Osmancik Formations. These formations illustrate the tectonic history of this portion of the basin as folding, ascent on the left side and descent on the back side of horizons that was caused by the formation of the pull-apart basin. Also, this portion of the basin was initially formed as a forearc basin by compressional forces in the Miocene and this tectonic environment created anticlines, as imaged by the seismic modeling. The anticlinal structure also contains the Osmancik and Danismen Formations which, according to well log analyses, have hydrocarbon potential. This possible reservoir zone has the potential to contain hydrocarbon reserves within this structural trap.

The potential reservoir zones were defined from well logs for the Well 2 and 3 wells but the reservoir zone that is between 1,760 and 1,775 meters on the Well 2 well can be described as a main reservoir zone because the cross-over using NPHI and RHOB logs size is bigger than other wells. However, reservoir petrophysical features results do not support economic and high hydrocarbon accumulation on the area. The gravity anomaly maps show that the study area has lower sedimentary thickness in comparison with the area surrounding it. The seismic reflection models, well log data analysis and gravity anomaly maps reveal that the basin has potential hydrocarbon accumulation but it might not be economical for conventional hydrocarbon production methods.

REFERENCES

Archie, G., 1942, The electrical resistivity log as an aid in determining some reservoir characteristics, Shell Oil Company: Society of Petroleum Engineers, p. 50-55, doi: 10.2118/942054-G.

Ates, A., and Kearney, P., 1999, New gravity and magnetic anomaly maps of Turkey: Research Notes, Geophys. J. Int., v. 136, p. 499-502, doi: 10.1046/j.1365-246X.1999.00732.x.

Balmino, G., Vales, N., Bonvalot, S., and Briais, A., 2012. Spherical harmonic modelling to ultra-high degree of Bouguer and isostatic anomalies: Journal of Geodesy, v. 86, p. 499-520, doi: 10.1007/s00190-011-0533-4.

Bedi, Y., Ergen, A., Dogan, A., Tekin, K., Ivanova, D., Bozkurt, A., Tuncay, E., Okuyucu, C., Soycan, H., and Goncuoglu, C., 2013, Stratigraphy and new ages from the Jurassic cover of the Istranca crystalline complex (Np.W Turkey): 66th Geological Congress of Turkey, Abstract Book, p. 82-83.

Blakely, J., and Simpson, W., 1986, Approximating edges of source bodies from magnetic or gravity anomalies: Geophysics, v. 51, p. 1494–1498, doi: 10.1190/1.1442197.

Blakely, J., 1996, Potential theory in gravity and magnetic applications: Cambridge University Press, p. 184-186.

Bonvalot, S., 2012, Commission for the geological map of the World: World Gravity Map.

Bozkurt, E., 2003, Origin of NE-trending basins in western Turkey: Geodinamica Acta, v. 16, p. 61-81, doi: 10.1016/S0985-3111(03)00002-0.

Brown, R., 2004, Interpretation of three-dimensional seismic data: American Association of Petroleum Geologists and the Society of Exploration Geophysicists, v. 9, p. 541-542.

Burkan, K., 1992, Geochemical evaluation of the Thrace basin, in Proceedings of the ninth petroleum congress of Turkey: Chamber of Petroleum Geology of Turkey, TPAO, v. 9, p. 34–48.

Caldwell, C., 1997, Exploring for stratigraphic traps: Oil field review, Schlumberger Company, p. 48-58.

Conybeare, D., Cannon, S., Karaoguz, O., and Uygur, E., 2004, Reservoir modelling of the Hamitabat field, Thrace basin, Turkey: an example of a sand-rich turbidite system, confined turbidite systems: Geological Society, Special Publication, v. 222, p. 307–310.

Cordell, L., 1979, Gravimetric expression of graben faulting in Santa Fe country and the Espanola basin, New Mexico: Geological Society Guidebook, 30th Field Conference, p. 59–64.

Coskun, B., 1996, Oil and gas fields-transfer zone relationships, Thrace basin, NW Turkey: Marine and Petroleum Geology, v. 14, p. 401–416, doi: 10.1016/S0264-8172(96)000621.

Datri, A., Zuffa, G., Cavazza, W., Okay, A., and Vincenzo, G., 2012, Detrial supply from subduction / accretion complexes to the Eocene-Oligocene post-collisional southern Thrace basin (NW Turkey and NE Greece): Sedimentary Geology, v. 243-244, p. 117–129, doi:10.1016/j.sedgeo.2011.10.008.

Demir, D., Bilim, F., Aydemir, A., and Ates, A., 2012, Modelling of Thrace basin, NW Turkey using gravity and magnetic anomalies with control of seismic and borehole data: Journal of Petroleum Science and Engineering, v. 86-87, p. 44-53, doi: 10.1016/j.petrol.2012.03. 013.

Derman, A., 2014, Petroleum system of Turkish basins, Petroleum system systems of the Tethyan region: American Association of Petroleum Geologists, v. 106, p. 469-504, doi: 10.1036/13431864M106395.

EIA, 2015, Turkey is an increasingly important transit hub for oil and natural gas supplies as they move from Central Asia, Russia, and the Middle East to Europe and other Atlantic markets. https://www.eia.gov/beta/international/analysis.cfm?iso=TUR

Elmas, A., 2011, The Thrace Basin: stratigraphic and tectonic paleo-geographic evolution of the Palaeogene formations of northwest Turkey: International Geology Review, v. 54, p. 1419-1442, doi: 10.1080/00206814.2011.644732.

Gorur, N., and Okay, I., 1996, A fore-arc origin of the Thrace basin, NW Turkey: Geology Rundsch, v. 85, p.662-668, doi: 885:662-668.

Grauch, V., and Cordell, L., 1987, Limitations of determining density or magnetic boundaries from the horizontal gradient of gravity or pseudo gravity data: Geophysics, v. 52, p. 118–121. doi: 10.1190/1.1442236.

Gurgey, K., 2009, Geochemical overview and undiscovered gas resources generated from Hamitabat petroleum system in the Thrace Basin, Turkey: Marine and Petroleum Geology, v. 26, p. 1240–1254, doi:10.1016/j.marpetgeo.2008.08.007.

Hamada, M., 2004, Reservoir Fluids Identification Using Vp/Vs Ratio: Oil and Gas Science and Technology, v. 59, p. 649-654, doi: 10.2516/ogst:2004046.

Hart, B., 2000, 3-d seismic interpretation, A Primer for Geologists: Society for Sedimentary Geology, Short Course Notes, v. 48, p. 77-96.

Hearst, J., Nelson, P., and Paillet, F., 2000, Well logging for physical properties, A Handbook for Geophysicists, Geologists, and Engineers, Second Edition.

Herron, A., 2011, First Steps in Seismic Interpretation: Society of Exploration Geophysicists, p. 9-20, doi: 10.1190/1.9781560802938.fm.

Hinsberger, D., 2010, A key extensional metamorphic complex reviewed and restored: The Menderes massif of western Turkey: Earth Science Reviews, v. 102, p.60-76 doi: 10.1016/j.earscirev.2010.05.005.

Islamoglu, Y., Harzhauser, M., Gross, M., Moreno, G., Coric, S., Kroh, A., Rogl, A., and Made, J., 2008, From Tethys to Eastern Paratethys: Oligocene depositional environments, paleoecology and paleobiogeography of the Thrace basin (NW Turkey): Int J. Earth Sci. (Geol Rundsch), v. 99, p. 183-200, doi: 10.1007/s00531-008-0378-0.

Jacobsen, H., 1987, A case for upward continuation as a standard separation filter for potential field maps: Geophysics, 52, p. 1138–1148.

Jain, P., 2012, Identification of gas using Vp/Vs vis-a-vis Poisson’s ratio: 9th Biennial International Conference & Exposition on Petroleum Geophysics, Poster Study.

Kazei, V. V., Troyan, V. N., Kashtan, B. M., and Mulder, W. A., 2013, On the role of reflections, refractions and diving waves in full-waveform inversion: Geophysical Prospecting, v. 61, p. 1252-1263, doi: 10.1111/1365-2478.12064.

Kern, H., 2011, Measuring and modeling of p- and s-wave velocities on crustal rocks: A key for tthe interpretation of seismic reflection and refraction data: International Journal of GGeophysics, v. 3, p. 1-9, doi: 10.1155/2011/530728.

Keskin, C., 1971, Geology of the Pinarhisar Thrace basin, Turkey: Geology magazine Turkey, v. 14/1, p. 31-84.

Keskin, C, 1974, Stratigraphy of north Ergene, Thrace basin, Türkiye: Second Petroleum congress, Ankara, v. 2, p. 137-163.

Kilias, A., Falalakis, G., Sfeikos, A., Papadimitriou, E., and Vamvaka A., 2011, Architecture of Kinematics and Deformation History of the Tertiary Supradetachment, Thrace Basin: Rhodope Province (NE Greece): New Frontiers in Tectonic Research, v. 3, p. 242-263, doi: 10.5772/20276.

Kim, Y., Cho, Y., and Shin, C., 2013, Estimated source wavelet-incorporated reverse-time migration with a virtual source imaging condition: Geophysical Prospecting Supplement, v. 61, p. 317-333, doi: 10.1111/j.1365-2478.2012.01119.x.

Larionov, V., 1969, Radiometry of boreholes, NEDRA, Moscow.

Lu, L., 2014, Seismic depth imaging in anisotropic media East Coast of Canada case study: Department Of Geoscience Calgary Alberta, Master Thesis.

Luthi, S., 2000, Geological well logs, in reservoir modelling: Springer.

Okay, A., Ozcan, A., Imren, C., Boztepe, A., Demirbag. E., and Kuscu, I., 2000, Active faults and evolving strike-slip basin in the Marmara Sea, northwest Turkey: a multichannel seismic reflection study: Tectonophysics, v. 321, p. 189–219, doi: 10.1016/S0040-1951(00)00046-9.

Pace, P., Scisciani, V., and Calamita, F., 2012, Positive flower structures as reactivated normal faults long obliquethrust ramps: examples from the Apulian structures: Central-SouthernApennines, Online Soc. Geol., v. 21, p. 47 -49.

Patel, D., Giertsen, C., Thurmond, J., Gjelberg, J., and Eduard M., 2008, The seismic analyzer: interpreting and illustrating 2-D seismic data: Ieee Transactions on Visualization and Computer Graphics, v. 14, p. 1551-1572, doi: 1077-2626/08.

Pavlis, N.K., Holmes, S.A., Kenyon, S.C., and Factor, J.K., 2012. The development and evaluation of the Earth gravitational model 2008 (EGM2008): Journal of Geophysical Research: Solid Earth, v. 117, p 406-430, doi: 10.1029/2011JB008916.

Perincek, D., 1991, Possible strand of the North Anatolian Fault in the Thrace basin, Turkey – an interpretation: Aapg Bulletin, v. 75, p. 241–257, doi: 10.1306/0C9B2795-1710-11D7-8645000102C1865D.

Perincek, D., Atas, N., and Karatut, S., 2015, Geological Factors Controlling Potential of Lignite Beds within the Danismen Formation in the Thrace Basin: Bulletin of the Mineral Research and Exploration, v. 150, p. 77-108.

Rider, M., 1991, The geological interpretation of well logs, Revised Edition: Petroleum Exploration Consultant Rider-French Consulting Cambridge and Sutherland.

Rivas, J., 2009, Gravity and magnetic methods: Short Course on Surface Exploration for Geothermal Resources.

Saner, S., 1980, Batı Pontidlerin ve komsu havzalarin olusumlarinin levha tektoniği kuramiyla aciklanmasi, Kuzeybati Türkiye: MTA Dergisi, v 93-94, p. 1-19.

Schindler, C., 1997, Active tectonics of northwestern Anatolia – The Marmara Poly-Project, A Multidisciplinary Approach by Space-Geodesy, Geology, Hydrogeology, Geothermics, and Seismology.

Schlumberger, 1994, Neutron Porosity Logging Revisited: Oil Field Review, https://www.slb.com/~/media/Files/resources/oilfield_review/ors94/1094/

Schuck, A., 2007, Environmental Geology: Handbook of Field Methods and Case Studies, doi: 10.1007/978-3-540-74671-3.

Sen, S., and Yıllar S., 2009, The Korudağ anticlinorium in the south Thrace basin, Northwest Turkey: A Super Giant Petroleum Trap Complex: Aapg Bulletin, v.93, p. 465-485, doi: 10.1306/09290808072.

Sen, S., 2011, Petroleum source rock assessment of the south western Thrace basin, Nw Turkey: Energy Sources, v. 33, p. 1005-1017, doi: 10.1080/15567036.2010.485177.

Sengor, A., and Yilmaz, Y., 1981, Tethyan evolution of Turkey, a plate tectonic approach: Tectonophysics, v. 75, p. 181-241, doi: 0040-1951/81/0000.

Sheriff, E., 1994, Encyclopaedic dictionary of exploration geophysics: 3rd edition, Society of Exploration Geophysics, p. 129-155, doi: 10.1190/1.9781560802969.chf.

Siyako, M, 2006, Trakya bolgesi litostratigrafik birimleri, Stratigrafi Komitesi: MTA, v. 2, p. 59-62.

Siyako, M., and Huvaz, O., 2007, Eocene stratigraphic evolution of the Thrace basin, Turkey: Sedimentary Geology, v. 198, p. 75-91, doi: 10.1016/j.sedgeo.2006.11.008.

Soylu, C., Harput, B., Illiez, I., Erturk, O., Iztan, H., Ugur, A., Goker, T., Harput, A., Gurgey, K., and Sayılı, S., 1992, Organic geochemical evaluation of the Northern Thrace basin: Proceedings of the Ninth Petroleum Congress of Turkey, Chamber of Petroleum Geology of Turkey, TPAO, v. 9, p. 49–61.

Stieber S., 1970, Pulsed neutron capture log evaluation: Louisiana Gulf Coast - Spe Fall Meeting Aime, Conference Paper, doi: 10.2118/2961-MS.

Temel, O., and Ciftci, N., 2002, Stratigraphy and depositional environments of the Tertiary sedimentary units in Gelibolu peninsula and islands of Gökçeada and Bozcaada (Northern Aegean Region): TAPG Bull, v. 14, p. 17–40.

TPAO, 2015, Basic activities, Production, http://www.tpao.gov.tr/eng/?tp=m&id=79.

Turgut, S., Siyako, M., and Dilki, A., 1983, The geology and the petroleum prospects of the Thrace Basin: Proc. Geol. Congr. Turkey, v. 4, p. 35–46.

Turgut, S., Turkaslan, M., and Perincek, D., 1991, Evolution of the Thrace Sedimentary Basin and Its hydrocarbon prospectivity, in Generation, Accumulation, and Production of europe's Hydrocarbons: edited by A. M. Spencer, Oxford University Press, v. 1, p. 415–437.

Unal, O., 1967, Trakya jeolojisi ve petrol imkanlari: Turkiye Petrolleri Anonim Ortakligi Arama Grubu Rapor, v. 391, p.102.

Usumezsoy, Ş., 1982, Istranca Masifinin Petrojenetik Evrimi: İstanbul Üniversitesi Yerbilimleri Fakültesi, Doktora Tezi.

Van Krevelen, D.W., 1984, Organic geochemistry—old and new: Organic Geochemistry, v. 6, p. 1-19.

White, R., Simm, R., 2003, Tutorial: Good practice in well ties: EAGE first break, v. 21, p. 75–83.

Yildiz, A., Toker, V., and Enguler, İ., 1997, The nanno-planktonbiostratigraphy of the Middle Eocene−Oligocene units in southern the Thrace Basin and surface water temperature variations: Türkiye Petrol Jeologlari Derneği Bülteni, v. 9, p. 31−44.

Yilmaz, O., 1987, Seismic data processing, Society of Exploration of Geophysics – Investigations in Geophysics, v, 2, p. 1001-1212, doi: 10.1190/1.9781560801580.ch7.